ZEUS PROGRESS REPORT

ZEUS UK COLLABORATION

May 2000

Contents

ZEUS Progress Report

ZEUS UK Collaboration

1 Introduction

Since the last ZEUS report to the PPESP, HERA luminosity running restarted in August 1998 after a shutdown earlier in the year to improve the e^- beam lifetime and to increase the proton beam energy from 820 to 920 GeV. HERA then ran in e^-p mode, for the first time since 1994, until mid 1999 when e^+p running was resumed. It may be noted that, as from January 1999, the performance of HERA improved owing to a better understanding of the machine and the ZEUS data-taking efficiency was in excess of 80% for both e^- and e^+ running. The total e^- (e^+) luminosity delivered to ZEUS over this period, up to late April 2000, was about 24.8 pb^{-1} (57.5 pb^{-1}) of which 17.4 pb^{-1} (44.5 pb^{-1}) were recorded by ZEUS. This data sample is now being analysed although many of the physics results reported here are based on the 44.5 pb^{-1} of data taken up to 1997.

The UK groups continue to have responsibility for the operation and maintenance of the Central Tracking Detector (CTD) which was built in the UK and is equipped with trigger and read-out electronics designed and manufactured in the UK. It is essential that we continue to have the resources to maintain the performance of the CTD at its present high standard since the tracking information it provides is vitally important for ZEUS triggering and for all physics analyses. (ZEUS data-taking is inhibited unless the CTD is active.)

HERA will be shutdown for a major upgrade in September 2000 and is expected to restart in June 2001 with greatly improved luminosity and the possibility of running with longitudinally polarised e^- and e^+ beams. The new MicroVertex Detector (MVD), in which the UK is playing a significant role, and the Straw Tube Tracker, which will significantly improve the forward tracking, are to be installed in the shutdown. The UK is also involved in the provision of a new polarimeter for measurement of the electron or positron beam polarisation. The increase in luminosity together with polarised beams will give access to quantitative electroweak physics at large Q^2 and increase the discovery potential of HERA to effects beyond the standard model.

This report is structured as follows: CTD status and infrastructure are covered in section 2, the UK contributions to the MVD in section 3, the polarimeter upgrade in section 4, physics results with ZEUS UK involvement in section 5 and future plans and resources requested in section 6. Lists of publications, theses and the membership of ZEUS-UK groups are contained in the appendices. ZEUS UK physicists continue to hold important positions in the management and leadership of the experiment as shown by the organogram in appendix G.

2 Central tracking detector status and infrastructure

The Central Tracking Detector (CTD) is a large volume cylindrical drift chamber covering the central region ($15^\circ < \theta < 164^\circ$). It provides charged particle tracking, momentum measurement and identification through dE/dx. It also participates in all three levels of the ZEUS trigger.

The CTD's 4608 sense wires are arranged in nine superlayers; superlayer one being the innermost. The wires in odd-numbered superlayers run parallel to the chamber axis, whilst those in the even-numbered layers have a small stereo angle ($\approx 5^\circ$). Taken together they provide sufficient information to reconstruct tracks in three dimensions. All wires in the chamber are equipped with Flash Analogue-to-Digital Conversion (FADC) electronics and, in addition, all wires in superlayer one and the odd numbered wires in superlayers three and five have z-by-timing readout for the first-level trigger.

The CTD readout has performed very reliably over the last two years. Dead channels remain at no more than 2%. The chamber resolution and efficiency have remained stable for the last six years. As we approach the HERA upgrade we are confident that the chamber readout electronics will continue to perform reliably for the lifetime of the experiment.

2.1 Triggering

ZEUS operates a three-level trigger, of which the first level is a hardware-based system whose principal aim is to reduce backgrounds that do not come from the interaction point. CTD information is essential for this and the detector uses dedicated, pipelined processor cards which provide tracking data to the global first-level trigger. The CTD first-level trigger has operated reliably throughout the last two years.

The ZEUS global second-level trigger uses more precise software algorithms to clean the event sample further and classify certain classes of physics events. Detailed tracking information is provided by the CTD second-level trigger which makes use of the data from all five axial superlayers and the z-by-timing information from layers 1, 3 and 5. A precise measurement of the event vertex at the second level is a powerful technique for rejection of background. In preparation for the HERA upgrade and the forthcoming microvertex detector, modifications have been made to the CTD transputer network to allow data from the FADC electronics to be sent to the proposed Global Tracking Trigger. This system will combine CTD data with the very precise tracking information from the microvertex detector, allowing a very accurate event vertex measurement with the possibility to tag long-lived particles.

The third-level trigger (TLT) runs on Unix workstations using an appropriate version of the off-line reconstruction code. The CTD TLT code is an optimised version of the full off-line reconstruction. Its performance is only slightly below that of the off-line version and aids monitoring of the system by providing early warning of any changes in critical CTD parameters.

2.2 Infrastructure, Slow Control and Monitoring

The advent of the year 2000 necessitated some changes to the CTD online computer systems. At the end of 1999 the old VAX-VMS computers used for the CTD run-control and monitoring systems were replaced with new AXP-OpenVMS workstations that are fully Y2K compliant. The new systems have operated continuously since their installation without problems.

Online data-quality monitoring (DQM) is an important issue. ZEUS has adopted an approach whereby simple DQM checks are performed automatically and the shiftcrew notified if any problems are found. The CTD DQM system is, therefore, being updated to work in this new framework. More detailed, off-line DQM checks are still performed by the automatic job-submission system that has been used for the last few years. This system has proven to be most effective, both in terms of efficient utilisation of manpower and timely diagnosis of problems on the chamber.

In general the support infrastructure for the CTD has performed well. There have been two incidents connected with the chamber cooling system where the narrow water pipes clogged with copper residue. The first incident was solved by reversing the water flow though the cooling pipe, flushing out the blockage. However, since the pressure of the cooling water supply to the CTD was reduced in 1999 there has been an increased tendency for the pipes to block. To remedy this a new booster pump has been purchased in conjunction with the DESY cooling water group. This pump will increase the input water pressure to the local CTD cooling loop thus increasing the water flow. It is hoped that this measure, in conjunction with a fine filter on the CTD cooling water input line, will remedy any potential future problems. In any case, the cooling circuit will be thoroughly checked in the upcoming long shutdown.

The continued operation and reliability of the CTD is of utmost importance to ZEUS. The CTD has operated reliably without causing any significant down-time for the experiment for almost ten years. However, in recent months there have been many instances of repeated trips of the high voltage (HV) in the outer superlayers. The only way to recover the affected parts of the chamber has been to disable the HV to that region for typically a few days before attempting to switch it on again. It should be stressed that the problems to date have been confined to superlayers eight and nine which play no part in the first-level trigger. The impact on the second- and third-level triggers is small. Extensive investigations have failed to show any correlation between the frequency of the trips and external environmental factors - including gas composition. The preliminary conclusion is that there is an effect in the chamber itself which causes the HV problems. To address this possibility, the CTD gas system has been modified to allow water to be added to the gas mix. This procedure has been successfully used in many other experiments and it is hoped that this simple solution will prove to be as effective for the CTD.

3 ZEUS Microvertex Detector

ZEUS UK groups at RAL, Oxford and UCL were originally involved in 3 aspects of the ZEUS microvertex detector (MVD) project: the clock and control electronics; online and offline alignment and installation.[1] Recently Glasgow has joined the offline alignment effort. For strong physics reasons and because of the experience of the UK groups in track triggers, we continue to give some support to the development of a global track trigger (GTT) which will eventually use hits from the MVD, CTD and forward trackers. This work, as well as our involvement in the off-detector electronics, is closely connected to the DAQ and slow control systems. As part of this effort, an integrated online event display and histogram presenter for MVD hits has been produced. Through discussions on installation procedures we now have responsibility for a cable patch box which has grown into a larger and more expensive task than anticipated. Because of a severe shortage of effort at RAL, UCL and Oxford had to take on more responsibility in the areas of clock and control and installation respectively. Before discussing the UK tasks in more detail a brief overview of the detector and project status is given.

In the two years since the last report from ZEUS to the PPESP, the MVD project has moved from the final stages of design to full scale production. The MVD consists of a central barrel section with 3 almost complete layers of silicon microstrip detectors and 4 forward wheels. Each layer provides readout in two coordinates, using two layers of microstrip detectors with readout pitch at right-angles. The barrel has a total of 600 individual detectors arranged on 30 ladders running parallel to the beam pipe. The wheels contain a total of 112 sensors. The silicon detectors are read out using the HELIX chip mounted adjacent to the detectors, a total of 1648 chips for the 20736 channels. The key design parameters of the MVD are: angular coverage $10^\circ - 170^\circ$; impact parameter resolution of $100\,\mu$m at 90°; two-track separation of $200\,\mu$m. The active planes of the vertex detector are mounted in a carbon fibre tube 2m long supported from the ends of the CTD.

[1] IC was also involved in the installation of the MVD but had to drop out early on.

The beampipe has a central section of Al-Be welded to forward and rear conical sections made of Al. The beampipe is not attached to the MVD. The total material in the barrel region is $8\%X_0$ of which 82% is from the silicon ladders and on board electronics.

The carbon fibre tube and precision flanges for mounting the ladders and wheels have been completed at NIKHEF where the detector is being assembled. Silicon module production is ongoing at DESY (the ladders will be assembled at NIKHEF and the wheels at DESY). The completed MVD will be taken to DESY in September for an extended full system test with readout electronics and all services. The MVD is scheduled to be installed in ZEUS towards the end of January 2001.

3.1 Clock and Control Electronics

The clock and control (C+C) system for the MVD distributes the HERA clock and the ZEUS first level triggers to the HELIX readout chips. It also contains logic to handle error conditions and busy signals from the GFLT and the MVD ADC system, and distributes calibration data from the slow control at the beginning of a run. The original proposal envisaged a split system with a "Masterbox" and "Slaves" positioned in the rucksack adjacent to the ADCs, dealing with the digital logic, and a "HELIX driver" system positioned close to the detector fanning out the signals from the masterbox and dealing with the calibration data. The masterbox system was the responsibility of UCL and the HELIX driver was to be designed and built by RAL. Owing to lack of resources at RAL, UCL took on responsibility for the whole system.

The Masterbox and Slave design remain largely unchanged, although the systems are now positioned closer to the detector (about 24m away) than originally envisaged, but further from the GFLT. This change was motivated by space requirements and the need to place the ADCs closer to the detector, and implied significant changes to the cabling scheme. The masterbox was successfully prototyped and the final master and slave system has now been built, tested at UCL and delivered to DESY, the first part of the MVD off detector electronics to be completed.

The HELIX driver has undergone substantial design modifications, principally driven by the need to drive the HELIX chips from 5m from the detector rather than the 10-20m originally intended. The fanout from the masterbox to 200 modules is still performed on a HELIX driver board which also interfaces with the slow control for calibration. This part of the clock and control remains largely unchanged from the original design, although it now sits about 24m from the detector, adjacent to the masterbox and ADCs. However, because of the difficulty in driving the CMOS signals to the HELIX chips, a current amplifier is required in the patch box.

3.2 Patch Box

The off-detector MVD electronics and services will be situated about 24 m away from the detector in 5 racks outside the HERA interlock and near to the main ZEUS electronics 'rucksack'. As the MVD will be installed in the centre of the existing ZEUS detector it will not be possible to access the rear end of the MVD to connect cables after installation. A cable 'patch box', located about 4 m from the MVD inside the space previously occupied by a compensator magnet, will provide a place where the 'short' cables from the MVD can be connected to the 'long' cables to the readout electronics and services. The box will also be the location of booster amplifiers needed to get satisfactory clock and control signals to the HELIX readout chips. This project was not explicitly part of the original ZEUS UK MVD bid to the PPESP. The UK became involved, initially only in an advisory capacity, because of our responsibility for the installation of the MVD. However we also have a particular interest in this project through our clock and control responsibilities. The HELIX chip requires both LVDS and CMOS signals for timing and control. This puts very stringent requirements on the quality of the signals and thus the type and quality of the cables that run between the MVD and the services racks. On the other hand it is of paramount importance to keep material to a minimum in the MVD itself. It has not proved possible to drive clock and control signals from the services racks to the MVD and thus the patch box will have to contain active amplification and shaping of the signals. It has become a vital part of the MVD project but unfortunately it has also become considerably more expensive than the original 'plug board' concept. This could not have been foreseen at the time of the original proposal as the choice of the readout chip had not been made. At the time of the MVD proposal in 1997 the ABCD chip with optical fibre readout was one of the favoured options. However it turned out that the HELIX chip (being developed for HERA-B and LHCb) was the only chip with the required functionality that could be modified for ZEUS in the short time available. We therefore request additional funds from the PPESP to complete the patch box as described in section 3.6.

3.3 Alignment

The purpose of the optical alignment system is to provide measurements of the position of the MVD support structure with respect to the CTD with precision of 20 μm or better. It will also measure distortions of the structure as a function of time, thus defining stable periods for offline alignment using track data. The alignment system is a development of the technique using transparent amorphous silicon diodes pioneered by the ATLAS group at MPI Munich. For ZEUS the size of the sensors has been reduced by a factor of 4 to $5 \times 5\,\mathrm{mm}^2$ and the laser wavelength increased from the optical to the infra-red to optimise transparency. The sensors are microstrip detectors with 16 strips (pitch 312 μm) in each of two perpendicular directions. The readout is a modification of the Munich system (EB 168-DPSD from EG&G) using an RS232 interface at the present time. A VME interface is being designed for the final system. In the Munich application the readout chip was bonded to the sensor by a few cm of kapton cable. This is not possible in the MVD and in fact the signals need to be taken about 24 m without amplification to the readout. Finding suitable low impedance minimal-mass halogen-free cables for this 'off-the-shelf' proved to be impossible so they had to be designed and fabricated in Oxford. This turned out to be quite a challenging project in its own right but may have wider applications [1]. Laser and sensor development work was performed using a 2 m long optical bench[2] in Oxford and included: definition and test of the laser and laser optics; studies on the intrinsic precision of the sensors; sensor calibration procedures; optical and signal studies with multiple sensors per beam. With all corrections, a position resolution (with respect to a precision x-y stage) of a few μm has been achieved, see figure 1. The full system components and minimal mass readout cables are being produced and tested in Oxford. Permanent installation in the MVD support tube will start in May. Because of the need to develop both the laser and the readout cable, the optical alignment system is more expensive than anticipated.

During assembly the MVD support tube will be open and each half-cylinder placed in a rigid support frame. The laser system will be used to track any movement of the support tube during this period. In December 1999 and again in March 2000, a reduced prototype system consisting of two laser beams, 6 sensors per beam and readout was taken to NIKHEF for initial tests. Various distortions of the support structure and carbon fibre tube were investigated and measured - see figure 2. The system worked very well and demonstrated that the support frame was not stiff enough. In the second test the support frame alone was

[2] This is roughly the length over which the laser will have to operate in the final system.

investigated, although it had been stiffened it still showed considerable movement when a torsion was applied at one end. This has now been rectified, but the tests demonstrated the usefulness of the alignment system.

The detailed alignment of the individual silicon wafers will be performed using track data. The alignment parameters will provide small corrections to the ideal geometry of the MVD silicon wafers. During assembly in NIKHEF the positions of the wafers on the support structure will be measured using two and three dimensional precision measuring machines. This information and input from the optical system will provide initial data for the offline alignment procedure. For simplicity in the ideal geometry it is assumed that the silicon wafers are flat. However this is not the case and considerable work has already been undertaken to measure their actual shapes. From the measurements the shapes of wafers before mounting are parameterised with an 8 parameter semi-cubic polynomial form. Investigations are underway to see if this shape is compatible with the measurements from the first few barrel ladders. Other studies have been started to find the optimum track data for generating the track offset residuals that will be used in the determination of the alignment parameters.

3.4 Track Trigger and MVD DAQ

As ZEUS UK groups have a lot of experience with track triggers, we contributed the studies for possible improvements to ZEUS track triggering after the upgrade. However it was made clear that the UK groups did not have sufficient resources to take responsibility for any new trigger. We did agree to make the FADC information that is sent to the existing CTD second level trigger (SLT) available to a new trigger and this was done last year by the addition of some extra transputer links to the readout and SLT transputer network. With the enormous increase in processing power of computers over the past 10 years and particularly commodity PCs, it is now possible to perform what then required sophisticated parallel processing on a single PC cpu. We have continued to provide some effort for the development of a new global track trigger (GTT). This has been done without compromising our commitment to the PPESP funded activities on the MVD. The project also offers excellent training opportunities for graduate students (which have been taken up by a UCL student). What has been achieved is a port of the existing CTD SLT algorithm from OCCAM (the transputer language) to C. In addition, the algorithm has been extended to include stereo wire information in place of that from the z-by-timing system and data transfer rate studies have been performed using a transputer to VME interface (originally designed by NIKHEF for the ZEUS global second level trigger) and a PC (the hardware provided by the ZEUS DESY group). Figure 3 shows the improved track-vertex resolution with the stereo data. The results are very encouraging and it has already been demonstrated that the single cpu algorithm with axial plus stereo data has a mean latency of less than 3 ms on a 450 MHz Pentium III PC, compared to ~ 12 ms for the present system.

Although we originally intended to provide the online software for the clock and control system, it turns out to be more efficient for this to be provided by the DESY-led MVD DAQ team. Instead we are providing an online histogramming and event display package for the MVD. This ties in well with our alignment and trigger activities and it will be an invaluable tool during the system tests before installation and during the first months of data taking in HERA.

3.5 Installation

The UK has the responsibility for installing the MicroVertex Detector and Beam Pipe as an assembly into the ZEUS experiment. This is scheduled to take place in late January

2001. Great familiarity with both new and existing apparatus in and around the central region of the ZEUS experiment is necessary. This includes the new beam-pipe, magnet systems and the MVD itself as well as existing detectors, the Central Tracking Detector (CTD), which was designed and built by UK groups, and other tracking chambers and calorimeters. The installation procedure and method has evolved over the past year during which there has been dialogue between the UK installation team, the MVD mechanical designers (NIKHEF), the Beam Pipe designers (DESY) and all relevant experts. Briefly, the MVD plus 'short' cables for readout and services will be rolled through the CTD using specially designed trolleys at either end to spread the load. The UK team consists of four people working (part time) on installation, one with overall responsibility from the Rutherford Appleton Laboratory, two from Oxford Nuclear Physics Dept where the detailed design and manufacture of the required hardware is being undertaken and one person from UCL who has responsibility for cable routing etc. Early in the ZEUS upgrade schedule measurements will be made on the CTD to confirm that the proposed installation procedure can take place safely. There is an alternative procedure, which will be used if necessary. Before shipment to DESY all installation hardware will have been tested on a mock-up to verify its capability and to enable the procedures to be practised.

3.6 Financial Summary and Request for Funds

To the end of FY 99/00 a total of £75.7k has been spent on the project (£52k alignment; £18.5k C+C; £5k installation). We estimate that to complete the project we require a further £17k for the alignment system, £38k for the C+C, £10k for installation and £34.6k for the patch box. Leaving aside the patch box which is additional to the original proposal, this gives a estimated total spend of £140.7k compared to the £120k granted by the PPESP. Most of the increase comes in the optical alignment system, the cost of the cable development and manufacture totals nearly £15k and the lasers also turned out to be significantly more expensive to develop than anticipated (£19k rather than £10k).

To complete the project we request that an additional £20k on the original £120k be allowed and that an extra £35k be granted for the patch box. Any remaining shortfall will be made up from within the ZEUS UK groups.

4 The HERA Polarimeter Upgrade

4.1 Overview

The determination of the cross sections for CC and NC DIS at high Q^2 using polarised electron and positron beams is of first importance in detailed studies of the Standard Model. At present there are no measurements of charged current (CC) deep inelastic scattering (DIS) using polarised charged lepton beams and the data on the polarisation dependence of neutral current (NC) DIS is limited to low Q^2. These measurements will be one of the primary objectives of the ZEUS collaboration after the HERA upgrade. The polarisation dependence of the NC and CC cross sections is a direct consequence of the chiral structure of the SM, hence, measurements of these cross sections will allow important tests of the electroweak (EW) sector of the Standard Model (SM) to be made [2]. Two key examples of such tests are highlighted below.

1. Search for Right-Handed Charged Currents:
   A comparison will be made of the cross section for CC scattering using left- and right-handed beams. This will allow the chirality of the CC weak interaction to be observed for the first time using charged lepton beams and as such will represent a significant

test of the Standard Model. For example, in one year's running, a model independent limit on the mass of a hypothetical boson, W_R, mediating CC reactions between right handed fermions can be set at the level of $\sim$ 400 GeV.

2. Measurement of the Light Quark Couplings to the Z-boson:
The full potential of electroweak measurements at HERA will be realised when data have been taken with each of the four charge/polarisation combinations. It is by detailed comparison of the polarised NC and CC cross sections that the couplings of the u- and d-quarks to the Z-boson can be extracted. For example, with 250 pb^{-1} per charge/polarisation combination the u-quark couplings to the Z-boson can be measured with a precision of 10%.

These measurements require that the polarisation be known with a precision of 1 - 2%. The present polarimetry at DESY yields a precision of only $\sim$4%, making an upgrade of the system essential [3].

At present the HERA polarimetry system consists of two polarimeters [4]. The first, the transverse polarimeter, TPOL, is located in the HERA West area. The second, the longitudinal polarimeter, LPOL, is situated in the HERA East area upstream of the HERMES experiment where a pair of spin rotators are installed. The spin rotators rotate the natural transverse polarisation of the electron or positron beam into longitudinal polarisation.

Both the TPOL and the LPOL employ a laser to provide a beam of circularly polarised light which is shone upon the lepton beam. The degree of polarisation may now be determined by detecting Compton photons back-scattered off the lepton beam. The principle of operation of the devices is different. The transverse polarisation is best determined by measuring the spatial, up-down, asymmetry of the back scattered photon, while the longitudinal polarisation is determined by measuring the energy asymmetry of the photons. The two photon detectors, therefore, are optimized to measure the spatial coordinate of a photon in the case of TPOL, or the energy of a photon in the case of LPOL. Both detectors exist and have been operating for a number of years.

The TPOL calorimeter is separated horizontally into two halves. The energy sharing between the upper and lower halves may be used to determine the impact position of a photon in the vertical direction. The up-down position asymmetry used to determine the polarisation relies on the conversion of the up-down energy asymmetry into a vertical position. This conversion is referred to as the '$\eta(y)$-transformation'. At present the uncertainty on the $\eta(y)$-transformation gives the largest contribution to the systematic error on the measurement of the transverse polarisation. A precise determination of the $\eta(y)$-transformation in situ during running will lead to a significant improvement in the precision of the measurement of the transverse polarisation. In order to determine the transformation precisely it has been proposed to install a pre-radiator, instrumented with a silicon micro-strip detector, in front of the TPOL calorimeter.

We are currently engaged in the commissioning and evaluation of a silicon microstrip prototype system. The prototype front-end board comprises a 1×1 cm^2 single-sided silicon strip detector with a pitch of 80 μm. The detector is read out with an APV25 amplifier/multiplexer chip [5]. The prototype front-end board, designed and built at Imperial College, has been operated successfully in a test stand controlled with a Macintosh computer running LabView. We are now developing a VME based readout system in order to put the prototype into the TPOL area at DESY.

4.2 A Position Detector for the POL2000 TPOL Upgrade

The TPOL calorimeter must measure both the energy and the impact position of the back-scattered Compton photon. The position is measured using the spatial, up-down, asymmetry of the energy deposited in the calorimeter via the $\eta(y)$-transformation. Since the precision of the transverse polarisation is directly related to the precision with which the impact point of the photon is measured it is important to determine the $\eta(y)$-transformation in situ during data taking. In order to achieve the required relative precision on the transverse polarisation a pre-shower detector with position resolution of $\sim 30\ \mu$m is required. The position detector will also allow the calorimeter to be centred precisely on the Compton photon beam.

Three technologies have been considered for the position detector; diamond, scintillating fibres and silicon microstrips. In the following we propose to design, construct and commission the TPOL position sensitive detector. Our contribution to the POL2000 project will be a the major part of the ZEUS contribution to the polarimetry upgrade. The following cost and man-power estimates are based on the assumption that a silicon strip detector, currently the technology of choice, will be used. The costs of the precision mechanical items and the off detector electronics are common to all detector technologies. Hence, we believe that we shall be able to provide the position detector for the TPOL within the budget detailed below should a technology other than silicon microstrips be chosen.

4.2.1 Silicon Detector and Readout

The position detector must work in a region of very high photon flux. We therefore propose to use radiation-tolerant silicon for both the detector and the front-end readout electronics. The detector will be a 5×5 cm^2 single-sided silicon microstrip detector with a strip pitch of 80 μm. We will read the detector out with five APV25 chips. The front-end readout will be controlled using a VME system via an I2C interface board and the clock and control signals will be generated using a suitably modified SEQSI board [6, 7].

Two options exist for digitising the signals from the front-end card. The costing below assumes that five Sirocco ADCs will be used [8]. It may be convenient, and appropriate, to use a fast VME based ADC board which is being developed as part of the POL2000 TPOL DAQ upgrade.

4.2.2 Precision Mechanical Support Structure

The silicon detector must be precisely positioned with respect to the calorimeter. In addition, we require a method by which the linearity of the position response can be calibrated at the level of 10 μm or better. We are currently considering how best to perform this calibration. It has been shown that the linearity of the response of the position detector can be achieved using a scintillating fibre. The fibre would be supported horizontally in front of silicon detector and moved in the vertical plane by means of a precision stage. Figure 4 shows a schematic diagram of the scintillating fibre support structure. We propose to construct the mechanical parts of this assembly. The calibration system (scintillating fibre, photo-detectors, readout and associated software) will be the responsibility of other ZEUS members of the POL2000 collaboration.

4.2.3 Estimated Costs, Man-Power Requirements and Time-scale

Estimates of costs have been based upon previous experience with ZEUS electronics and other projects. The total cost of £50,000 is broken down in table 1.

The principal complication in the design of the front-end board over the prototype board is the distribution of the clock and trigger to the five APV25 chips. We estimate that the cost of producing one front-end board to be £5000. It is essential that we produce at least

Front-End Electronics	
Two front-end boards (1 spare)	£10,000
Off-Detector Electronics	
VME Crate	£5,500
Processor	£7,500
Modified SEQSI board	£1,000
I2C board	£1,000
Five CAEN V686 (Sirocco) ADCs	£12,500
Precision Mechanics	
Precision stage, supports etc.	£8,000
Sundry	
Readout computer, power supplies, etc.	£5,000
Total	£50,000

Table 1: Breakdown of costing for the TPOL silicon microstrip position detector.

one spare board. The manpower required to design and fabricate the front-end board is estimated to be four man-months and will be provided by Imperial College.

Existing modules will be purchased to provide most of the off-detector electronics. The SEQSI board will however need to be modified in a relatively straightforward way to so that it runs synchronously with the HERA clock.

The category in table 1 labelled 'Sundry' contains estimates for high- and low-voltage power supplies, cables and a PC to control.

The manpower required to design and build the precision mechanical items is half a man year and will be provided by Imperial College. The slow control and read-out software for the linearity calibration device will be provided by other members of the collaboration.

The timescale is driven by the HERA shutdown which starts in September this year. Following a successful completion of the beam test of the prototype system this summer we estimate that the design, construction and commissioning of the final system can be performed before HERA resumes operation in June 2001.

5 Physics Results

ZEUS-UK physicists are involved in a broad range of physics analyses. Very roughly Bristol, IC, Oxford and RAL are involved in structure functions and high Q^2 studies, while Bristol, Glasgow and UCL cover the hadronic final states.

5.1 High Q^2 Neutral Current Physics

In deep inelastic Neutral Current (NC) scattering, a photon or a Z^0 may be exchanged between the incoming lepton and the proton. The cross section for NC scattering is

$$\frac{d^2\sigma^\pm}{dxdQ^2} = \frac{2\pi\alpha^2}{xQ^4}[Y_+F_2(x,Q^2) - y^2F_L(x,Q^2) \mp Y_-xF_3(x,Q^2)]$$

where $Y_\pm = 1 \pm (1-y)^2$ and the structure function F_2 can be decomposed into $F_2 = F_2^{EM} + F_2^{Weak} + F_2^{Int}$, where F_2^{EM} represents the contribution from γ-exchange, F_2^{Weak}, the contribution from Z^0 exchange, and F_2^{Int} the contribution from $\gamma - Z^0$ interference. The parity violating cross section xF_3, becomes significant at large x and Q^2.

ZEUS UK physicists have continued their leading role in studies of high Q^2 physics at HERA. In August 1998 HERA switched to running with electrons until the end of May 1999, delivering a luminosity of $16\,pb^{-1}$. This allows for the first time a high statistics measurement of the $e^-\,p$ high Q^2 NC cross sections. This permits the first comparison of the charge dependence of the NC cross section at high Q^2, showing the sensitivity to the contribution of Z^0 exchange. A preliminary analysis of the electron data up to the end of running in May 1999 has been presented at HEP99 (Tampere, Finland). Figure 5 shows the NC differential cross section $d\sigma/dQ^2$ for both electron and positron beams compared to the predictions from the standard model using CTEQ4D [9] parton densities. For high values of $Q^2 > 3000\,\mathrm{GeV}^2$ the e^-p cross section is seen to lie above the e^+p cross section. Figure 6 shows the differential cross section $d\sigma/dx$ for e^-p scattering for $Q^2 > 800GeV^2$ and figure 7 $d\sigma/dx$ for $Q^2 > 10\,000\,\mathrm{GeV}^2$. The effect of the positive interference of the photon γ and Z^0 can be clearly seen in the e^-p data from figure 7. It can also be seen that the e^-p cross section is larger than than the e^+p cross section.

A measurement of the double differential reduced cross section $\tilde{\sigma}$, where

$$\tilde{\sigma}_{NC}(x, Q^2) = \frac{1}{Y_+}\frac{xQ^4}{2\pi\alpha^2}\frac{d^2\sigma_{NC}}{dxdQ^2},$$

is shown in figure 8. The data are seen to be well described by the Standard Model predictions from CTEQ4D and MRST. Figure 8 shows the reduced cross section at fixed x as a function of Q^2 for the e^-p data set. For Q^2 values above $1000\,\mathrm{GeV}^2$ the e^-p reduced cross section is clearly seen to turn upwards, whereas the e^+p data (not shown) turns down. This is consistent with the Standard Model expectation in which one expects positive interference of the Z^0 exchange for e^-p scattering and negative interference for e^+p scattering.

The new high statistics e^-p data in combination with earlier e^+p data allows the first extraction of the proton structure function xF_3 at high Q^2 and x. (The data sets used for the extraction of xF_3 are $30\,\mathrm{pb}^{-1}$ of e^+p data taken in 1996/97 and $16\,\mathrm{pb}^{-1}$ of e^-p data taken in 1998/99.)

The extraction of xF_3 is shown in figure 9. Here the measured xF_3 is plotted in bins of Q^2 as a function of the scaling variable x and compared with the Standard Model expectations from CTEQ4D and MRST. It can be seen that the data are in good agreement with the Standard Model predictions.

The precision of the xF_3 measurement is comparable with the first extraction of F_2 from data taken in 1992. This measurement will clearly benefit from the increased data after the HERA luminosity upgrade. An improved measurement of xF_3 will impose a tighter constraint on the high x valence quark distribution which will play an important role in estimating very high energy processes at the LHC.

5.2 High Q^2 Charged Current Physics

In Charged Current (CC) deep inelastic scattering (DIS) the exchanged W-boson picks out specific quark flavours from within the proton. Thus e^+p CC DIS is sensitive to the d valence quark density at high x and the $\bar{u}$ (and $\bar{c}$) quark density at low x. By contrast, e^-p CC DIS is sensitive to the u valence quark density at high x and the $\bar{d}$ (and $\bar{s}$) quark density at low x. Hence by measuring the dependence of the CC DIS cross section on the charge of the lepton beam we are able to study flavour-specific parton densities directly.

In 1999 ZEUS published measurements of the single and double differential e^+p CC DIS cross sections based on 48 pb^{-1} of data taken during the years 1994-1997 [10]. The publication also contains a determination of the mass of the W boson, M_W. The double differential CC cross section may be written as

$$\frac{d^2\sigma^{CC}}{dx\,dQ^2} = \frac{G_F^2}{2\pi x}\left(\frac{M_W^2}{M_W^2+Q^2}\right)^2 \tilde{\sigma}$$

where the reduced cross section, $\tilde{\sigma}$, is given at leading order by $\tilde{\sigma} = \bar{u} + \bar{c} + (1-y)^2(d+s)$. The reduced cross section is plotted as a function of x at several fixed values of Q^2 in figure 10. The Standard Model (SM), evaluated with the CTEQ4D [9] parton density functions (PDFs), gives a good description of the data, although at the highest x values the measured cross sections lie above the CTEQ4D predictions. The ZEUS NLO QCD fit [11] also gives a good description of the data. At high x the ZEUS fit gives cross sections which are larger than those of CTEQ4D. Note that the high-Q^2 NC and CC data were not included in either the CTEQ4D fit or the ZEUS fit.

The absolute magnitude of the CC cross section is determined by the Fermi constant, G_F, and the PDFs, while the Q^2 dependence of the cross section includes the propagator term $[M_W^2/(M_W^2+Q^2)]^2$, which produces substantial damping of the cross section at high-Q^2. A fit to the measured differential cross section $d\sigma/dQ^2$, treating M_W and G_F as free parameters was performed in order to investigate the extent to which the SM gives a consistent description of the data. The point which gives minimum χ^2 ($\chi^2_{\rm min}$) is displayed in figure 11 as the triangle together with the 70% confidence level contour, determined using statistical errors only. The values of G_F and M_W obtained are in good agreement with those quoted by the PDG [12], implying the universality of the CC interaction over a wide range of Q^2. The mass of the exchanged boson may be obtained from the Q^2 dependence of the cross section by constraining the normalisation of the cross section to the SM value. The value of M_W determined from this 'propagator-mass' fit is

$$M_W = 81.4^{+2.7}_{-2.6}(\text{stat.})^{+2.0}_{-2.0}(\text{syst.})^{+3.3}_{-3.0}(\text{PDF})\ \text{GeV},$$

The value of M_W obtained agrees with the value of $M_W = 80.41 \pm 0.10$ GeV from the PDG fit, using time-like production of W-bosons at the Tevatron and at LEP. Since CC DIS represents space-like exchange, the result is complementary to measurements of M_W from $p\bar{p}$ or e^+e^- annihilation and constitutes an important check of SM consistency.

The analysis of the 16 pb^{-1} of e^-p data taken during 1998 and 1999 with a proton beam energy of 920 GeV is now well underway. Preliminary results based on 6 pb^{-1} of data were shown at the spring and summer conferences of 1999. Figure 12a shows the cross section $d\sigma/dQ^2$ for e^-p scattering. The SM expectation, evaluated with the CTEQ4D PDFs, gives a good description of the data. The effect of the increased proton energy is small, as can be seen by comparing the SM expectation evaluated for a proton energy of 820 GeV with the 920 GeV expectation. In figure 12b the ratio of the cross section for e^-p CC DIS to the cross section for e^+p CC DIS is plotted as a function of Q^2. The e^-p cross section is a factor 2 higher at $Q^2 = 1000$ GeV^2, rising to a factor 10 at the highest Q^2 measured. In the quark parton model, this is understood to be due to the W coupling to the higher u-quark density in e^-p scattering, while the dominant e^+p process is the W coupling to d-quarks with a $(1-y)^2$ suppression. Both the normalisation and rise with Q^2 agree with the expectations of the SM.

The analysis of the recent e^+p data taken with a proton beam energy of 920 GeV has started. All the data taken up to September 2000 will be combined to give the definitive $e^\pm p$ CC DIS cross sections from ZEUS using unpolarised lepton beams.

5.3 Structure Functions

ZEUS UK groups continue to be strongly involved in the measurement and analysis of structure functions and provided a physics group coordinator in this area during 1998.

The groups were also well represented in the relevant working groups at the 1998 Durham Phenomenology Workshop and the DIS99 Conference in Zeuthen. UK people took the lead in drawing together various phenomenological approaches to ZEUS F_2 data over the full range of Q^2 [13]. The impact of the 1994 ZEUS data on NLO DGLAP fits, including a full treatment of systematic errors, was examined with particular emphasis on the low x low Q^2 region. This was part of a wider study of the transition region from pQCD to soft physics as $Q^2 \to 0$. The paper includes plots of the two slopes $dF_2/d\ln Q^2$ ('Caldwell' plot) and $dF_2/d\ln(1/x)$ that are important in the study of the transition region. Figure 13 shows the singlet and gluon momentum distributions from the NLO fits as functions of x in different Q^2 bins. The figure shows the importance of the F_2 data at low x and Q^2 in reducing the error on the gluon distribution at low x. It also shows that at the lowest Q^2 ($1\,\mathrm{GeV}^2$) the gluon density is probably less than that of the sea quark, provided that the DGLAP approach is still valid. This result is not what one would expect from a conventional understanding of the QCD enhanced parton model and may indicate that contributions beyond DGLAP are becoming important. We continue to work on the extraction of the very high statistics F_2 data set from the HERA 1996/7 runs. This data will be the definitive measurement at low and medium Q^2 by the ZEUS experiment. It is hoped that the data will be published later this year. We are also involved in NLO QCD fitting of the data and other phenomenological analyses.

5.4 Event Shapes

A recent revival of interest in the study of event shape measurements has been prompted by theoretical developments in the understanding of hadronisation or power corrections. Here, perturbative QCD calculations are extended into the region of low momentum transfers using approximations to higher-order graphs. At HERA, the Q^2 scale can be varied over four orders of magnitude enabling power corrections (proportional to $1/Q^p$, where p is the power) to be studied in detail. The data are compared to theoretical expectations for the power corrections, characterised by an effective coupling $\overline{\alpha}_0(\mu_I)$ specified at the infra-red matching scale $\mu_I \simeq 2$ GeV, and NLO pQCD calculations, determined by $\alpha_s(M_Z)$.

The Breit frame is where the exchanged gauge boson in DIS is purely space-like. Viewed in this frame, the incoming QPM quark is back-scattered with equal and opposite momentum ($Q/2$). Event shapes have been measured in the direction of the struck quark, corresponding to the current region, which is directly analogous to one hemisphere of a purely time-like e^+e^- interaction. A series of event shape variables have been studied which have varying sensitivity to hadronisation/power corrections and are noted below. Thrust ($\tau = 1 - T_z$) and jet broadening (B) sum the longitudinal and transverse momenta, respectively, of individual particles along the photon axis. τ_c is also defined with respect to the reconstructed thrust axis, in order to compare directly with e^+e^-. Jet mass (ρ) and the C parameter sum the product of two particle momenta weighted by $1 - \cos\theta_{ij}$ and $\sin^2\theta_{ij}$, respectively. These variables are each measured in the current region of the Breit frame and are scaled by the total visible energy (E_{vis}).

Mean values of these event shapes haves been measured by ZEUS [14] which can be interpreted theoretically via

$$\langle F \rangle = \langle F \rangle^{\mathrm{pert}} + \langle F \rangle^{\mathrm{pow}}$$

where

$$\langle F \rangle^{\mathrm{pert}} = c_{1,F}(x,Q) \cdot \alpha_s(Q) + c_{2,F}(x,Q) \cdot \alpha_s^2(Q)$$

with $c_{1,F}(x,Q)$ and $c_{2,F}(x,Q)$ being calculable coefficients of pQCD determined by the DISENT NLO program with renormalisation/factorisation scales set at $\mu_R = \mu_F = Q$. The power corrections are proportional to $1/Q$ with

$$\langle F\rangle^{\text{pow}} = \mathcal{M}' \frac{a_F}{Q} \frac{16\mu_I}{3\pi}\left[\overline{\alpha}_0(\mu_I) - \alpha_s(Q) - \frac{23}{6\pi}\left(\ln\frac{Q}{\mu_I} + 1.45\right)\alpha_s^2(Q)\right].$$

Here a_F is a calculable F-dependent coefficient and $\mathcal{M}' = 2\mathcal{M}/\pi \simeq 0.95$ is a two-loop level refinement to the calculations called the Milan factor.

The measured mean event shape values versus Q are shown in Figure 14, where the data are compared to two-parameter fits in $\overline{\alpha}_0(\mu_I)$ and $\alpha_s(M_Z)$ using the NLO calculation plus power correction approach described above. Overall, a reasonable description of the data can be achieved, although the x-dependence of variables measured with respect to the photon axis, τ and B, is not well described. The major theoretical uncertainty is that due to the renormalisation scale, indicated by the shaded band.

The results of two-parameter fits to the ZEUS data are given in Figure 15. The correlation of $\overline{\alpha}_0(\mu_I)$ and $\alpha_s(M_Z)$ is high and negative for $\langle\tau\rangle$ but is less for other variables. In each case, the data for the means of τ, B, τ_C, C and ρ, are described reasonably well by the theory, with a value of the universal non-perturbative parameter $\overline{\alpha}_0(\mu_I)$ of $\simeq 0.5 \pm 20\%$ and a value of $\alpha_s(M_Z)$ close to the world average. There are, however, remaining theoretical uncertainties due to uncalculated higher-order x-dependent terms which appear to be especially significant for B. In conclusion, the theoretical approach works remarkably well and ongoing refinements will generate further insight into non-perturbative QCD mechanisms in the generation of hadronic final states at high energies.

5.5 Fragmentation in DIS

A comparison, in the Breit frame, is made of the fragmentation associated with the outgoing struck quark to that in the target region; the latter is associated with the initial state radiation from the incoming proton.

The distributions in $\ln(1/x_p)$ (where $x_p = 2p/Q$) are shown for both the target and current regions in figure 16 as a function of Q^2 and x. This analysis is restricted to values of the scaled momenta $x_p < 1.0$ so that similar phase space regions for the target and current can be compared. Thus the accepted part of the target region is only a small part of the complete phase space. The fitted curves shown are two-piece normal distributions to guide the eye. In contrast to the current region, the target region distribution does not fall to zero as $\ln(1/x_p)$ tends to zero. Although the magnitude of the single particle density at the peak position of the current region distribution grows by a factor of about three over the Q^2 range shown, the single particle density of the target distribution, at the x_p value corresponding to the peak of the current distribution depends less strongly on Q^2 and increases by only about 30%. In addition the $\ln(1/x_p)$ distribution shows no significant dependence on x when Q^2 is kept constant. In the target region the peak position of the $\ln(1/x_p)$ distribution increases more rapidly with Q^2 than in the current region; this is consistent with the behaviour expected from cylindrical phase space. The approximate Gaussian distribution of the MLLA predictions peaking at $\ln(1/x_p) \sim 1.5 - 2.5$ is not observed. We conclude that the target distributions are inconsistent with the MLLA predictions when used in conjunction with LPHD [15].

5.6 Azimuthal Asymmetries

In DIS, the distribution of the azimuthal angle, ϕ, (measured in the hadronic centre-of-mass frame) between the lepton scattering plane, defined by the incoming and outgoing lepton momenta, and the hadron production plane, defined by the incoming virtual boson and an outgoing hadron has been measured.

Figure 17 shows the distributions of the azimuthal angle of the leading hadrons. The four plots are made with increasing minimum transverse momentum, p_c, of the hadrons. It can be clearly seen that at higher p_c the events follow a $\cos 2\phi$ distribution. This is a clear prediction of perturbative QCD which has never before been observed.

5.7 Heavy Quark Physics

5.7.1 Charm Production in DIS

Heavy flavours, particularly charm, are produced copiously in DIS at the low x values available at HERA. The dominant production mechanism is the boson-gluon fusion (BGF) process, which in principle means that this channel offers another way of measuring the gluon density in the proton. Charm is identified by the decay chain $D^* \to D^0\pi^+$, $D^0 \to K^-\pi^+$ or $D^0 \to K^-\pi^-\pi^+\pi^+$ and as the combined branching ratios in the D^* and D decays are only a few percent, the measurement requires a large luminosity. Since the threshold region is explored at low Q^2 it is necessary to use the massive quark BGF formalism, which has been worked out to NLO. UK groups were involved with the recent ZEUS measurement of F_2^c using the 1996 and 1997 data with a combined luminosity of $37\,\mathrm{pb}^{-1}$ [16]. Totals of 2064 ± 72 and 1277 ± 124 events were found for the $K\pi$ and $K3\pi$ decay channels respectively, representing an order of magnitude increase over earlier measurements at HERA. Figure 18 shows F_2^c as a function of x in bins of Q^2. The steep rise at low x at Q^2 above $4\,\mathrm{GeV}^2$, seen in the full F_2 data, is very striking. The curves show the expectation of the NLO BGF process, with the gluon distribution from the ZEUS QCD fit referred to above and with $m_c = 1.4\,\mathrm{GeV}$. The largest contribution to the uncertainty shown for the calculation is from the uncertainty in charm mass, here a variation of ±0.2GeV was allowed. High statistics measurement of heavy flavour processes will be a major goal with the MVD after the upgrade.

5.7.2 Charm Production in Diffractive Scattering

Charm production in diffractive interactions is particularly important due to its sensitivity to the presence of gluons. Therefore, tagging charm is a powerful method to distinguish between different theoretical models of diffraction. The principle reactions of interest are photon dissociative reactions (in which the photon dissociates into a hadronic system whilst the proton remains intact). These events can be identified by the presence of a large rapidity gap between the hadronic system and the outgoing proton direction. As in DIS, charm was identified using D^* reconstruction and events were identified as diffractive if the rapidity gap was at least 2 units. Differential D^* cross sections have been measured using the combined 1995-97 data sample for the $D^* \to D^0\pi, D^0 \to K\pi$ decay and the 1996-97 data for the $D^* \to D^0\pi, D^0 \to K\pi\pi\pi$ channel. These cross sections are shown in figure 19 and figure 20 respectively. The fraction of D^*s that are diffractively produced has also been measured and is shown in figure 21.

5.7.3 Charm and Beauty Photoproduction

Charm quarks inside jets were measured via D^* decays at ZEUS in 1998 and published in 1999 [17], with UK physicists as principle authors. The results showed for the first time that charm is produced copiously in resolved photon events.

Heavy quarks can also be detected by identifying electrons from their decay. This is done by measuring the distinctive rate of energy loss of electrons in the CTD, as well as the way they interact in the calorimeter. Results by UK physicists from this method not only confirm the result of the D^* studies, but also show a significant production rate for beauty quarks as may be seen in figure 22. The beauty component is identified by measuring the transverse momentum of the electron relative to the jet axis since electrons from beauty decays are expected to have a harder p_t^{rel} spectrum owing to the mass of the b. The beauty fraction has been extracted by fitting the data distribution with Monte Carlo. Using this fraction the visible cross section can be compared to LO QCD models.

Existing measurements of open beauty production from both HERA and $p\bar{p}$ colliders show cross sections that are high when compared to standard NLO QCD predictions. A direct comparison of the ZEUS result with an NLO QCD prediction is also possible by using the Monte Carlo to extrapolate to the $b\bar{b}$ cross section in a limited kinematic region. This extrapolated cross section also lies above the theoretical prediction.

Understanding such results is an important test of QCD and a necessary step towards understanding the new physics potential of future colliders. The results also represent a substantial technical triumph in the operation and understanding of the CTD dE/dx readout, a UK responsibility from the beginning of ZEUS.

The presence of heavy quarks in the evolution of the photon structure offers a promising window for understanding the development of QCD structure, splitting functions and threshold effects. The ability at HERA to select concurrently on E_T^{jet}, photon virtuality and x_γ^{OBS}, as well as to compare heavy flavour jets with untagged jets, makes it uniquely suitable for detailed studies in this area. Thus heavy flavour jet production will be a growth area, and is a major driving force behind the UK's involvement in the MVD. The GTT will play a vital part in allowing these events to be saved at relatively low E_T^{jet} even after the upgrade, particularly if charm enrichment can be implemented.

5.8 Jet Production

Our studies of jets in photon-proton collisions at HERA continue to give information on the hadronic "structure" of the photon, and UK groups continue to lead these analyses. Since the last report we have measured [18] the dynamics of three jet production with higher statistics than our previous measurement [19] and shown explicitly the effects of the colour of the incoming quarks and gluons (see figure 23) which is a fundamental test of the strong interaction. We have also measured the dijet angular distributions with high statistics and at high E_T^{jet}.

Although these studies present a reassuring picture of jet photoproduction in that the dynamics are well described by QCD, there is clear and growing evidence for a significant discrepancy in the rate of resolved photon interactions, with the data lying above the NLO QCD expectations by around 30%. We have measured cross sections differential in η^{jet}, E_T^{jet} and x_γ^{OBS}, the fraction of the photon's momentum entering the hard subprocess. In all cases, although the direct-photon dominated high x_γ^{OBS} region agrees well with the theory, the resolved-photon dominated low-x_γ^{OBS} region shows an excess as may be seen in figure 24. The current evidence points to the photon structure as the source of this discrepancy. ZEUS is sensitive to the photon structure in a Q^2 region not measured by LEP. We are continuing work on reducing the systematic uncertainties in the measurements and evaluating the implications for photon structure and QCD.

5.9 Inclusive Prompt Photon Photoproduction

Further progress has been made in studying photoproduction processes in which a high-E_T photon is emitted. Such photons may be produced directly as part of the QCD hard scattering subprocess, and are known as prompt photons. In a first ZEUS paper [20] the observation of such processes was first confirmed at HERA and the basic characteristics of events with a prompt photon and a counterbalancing jet were established. In a more recent paper [21] the properties of inclusive prompt photons have been studied.

High energy photon production can be described as a sum of direct processes, dominated by the elastic scattering of the incoming photon off a quark in the proton, and resolved processes, in which the incoming photon is a source of partons which subsequently scatter. A source of photons which it is desirable to minimise comes from dijet processes in which a final state quark hard-radiates a photon, referred to radiative events. The requirement that the final-state photon be relatively isolated from other final-state particles reduces the radiative contribution and also neutral-meson backgrounds. The latter are finally subtracted off by means of signal-shape properties in the ZEUS barrel calorimeter.

Figure 25a shows the transverse energy of the prompt photons observed by ZEUS, compared with various theoretical predictions, for photon pseudorapidities in the range plotted in figure 25b. Here, the pseudorapidity η^γ of the photon is plotted for photons in the E_T range 5-10 GeV. LG denotes the NLO theory of Gordon; K&Z denotes that of Krawczyk and Zembruski. The two figures show that the transverse energy is well predicted on average by most of the theories, although HERWIG is a little low. However the observed pseudorapidity of the photons is higher than all the theories in the rear region, although the statistical significance is not large. This may requires further theoretical input.

We plan to improve these measurements by using the considerably increased statistics that are now becoming available, and by improving our techniques to include photons in the forward and rear calorimeters as well as the barrel. At the same time, we are engaged in an analysis of the intrinsic k_T of partons in the proton, which can be probed by means of the kinematics of events with a prompt photon and a jet. This is in response to a number of prompt photon measurements mainly from Fermilab, which seem to imply surprisingly large values of this quantity. Further planned analyses include a study of prompt photons in DIS events.

This entire area of study will be further enhanced by the very much improved luminosities available after the HERA upgrade.

6 Future Plans and Resources Required

The first phase of HERA running, prior to the high luminosity upgrade has established HERA as the place to study proton structure in the hitherto unexplored region of low-x and, increasingly, to test assumptions made at high-x. The HERA upgrade programme has been planned such the envisaged shut-down is ten months from September 2000 to June 2001. The upgrade will enable luminosities to be increased by a factor five from those currently available and will extend the range of QCD and electroweak analyses which can be performed, as well as enhancing search capabilities beyond the Standard Model.

The ability to tag heavy flavours using the MVD and the ability to precisely measure the polarisation of the lepton beams using the TPOL will greatly improve these studies. The future programme builds upon existing ZEUS-UK analyses as well as the investment in the MVD and planned work on the TPOL. The maintenance of the quality of data from the CTD will remain a priority. Over the next two years we will have completed the installation of the MVD and the TPOL, subject to approval, and will start a new phase of high-luminosity investigations. The funds requested are £50,000 to design and build the TPOL, £20,000 to complete the original MVD proposal and £35,000 to complete the patch box for the MVD. We note that the HERA programme will last until at least 2005 and this investment, as part of the HERA upgrade, represents a key input to the exploitation of the rich harvest of physics made possible by high luminosity and polarisation.

References

[1] PPARC Frontiers Magazine Jan 2000.

[2] Proceedings of the workshop on 'Future Physics at HERA', eds. G. Ingelman, A de.Roeck and R. Klanner, DESY 1996.

[3] V. Andreev et al., *A Proposal for an Upgrade of the HERA Polarimeters for HERA 2000*, DESY-PRC-99-04.

[4] V. Andreev et al., *POL2000: Status and Plans: An Appendix to the POL2000 Proposal*, DESY-PRC-99-05.

[5] APV25 Users Guide, http://www.te.rl.ac.uk/med/apv25_web/user_guide.html

[6] E. Murer, VI2C, VME I2C Users Manual

[7] M. Morrissey, SEQSI Users Manual

[8] G. Claus, W. Dulinski and A. Lounis, CRN-96-33.

[9] H.L. Lai et al., Phys. Rev. D 55 (1997) 1280.

[10] J. Breitweg et al., Eur. Phys. J. C 12 (2000) 411.

[11] M. Botje, DESY 99-038, NIKHEF-99-011.

[12] Particle Data Group, C. Caso et al., Eur. Phys. J. C 3 (1998) 1.

[13] ZEUS Collaboration, J. Breitweg et al., Eur. J. Phys. C 7 (1999) 609-630.

[14] R. Waugh, Glasgow University Ph.D. Thesis (1999); G. McCance, "Event Shapes at HERA", Moriond Proceedings (in preparation).

[15] ZEUS Collaboration, J. Breitweg et al., DESY 00-040 (March 2000), accepted by Physics Letters B - PLB 15927.

[16] ZEUS Collaboration, J. Breitweg et al., Eur. J. Phys. C 12 (2000) 35-52.

[17] ZEUS Collaboration, J. Breitweg et al., Eur. Phys. J. C 6 (1999) 67-83.

[18] E.A.Heaphy, *Three-jet Production at HERA*, Durham Workshop on Collider Physics, Sept. 1999.

[19] ZEUS Collaboration, J. Breitweg et al., Phys. Lett. B 443 (1998) 394-408.

[20] ZEUS Collaboration, J. Breitweg et al., Phys. Lett. B 413 (1997) 201.

[21] ZEUS Collaboration, J. Breitweg et al., Phys. Lett. B 472 (2000) 175.

Appendices

A ZEUS Journal Publications

(Published since the PPESP report March 1998)

1. A. Quadt et al., *The Design and Performance of the ZEUS CTD Second Level Trigger*, Nucl. Instr. Meth. A438 (1999) 472-501.
2. ZEUS Collaboration; J.Breitweg et al. *High-E_T Inclusive Jet Cross Sections in Photoproduction at HERA.* The European Physical Journal C4 (1998) 591-606
3. ZEUS Collaboration; J.Breitweg et al. *Diffractive Dijet Cross Sections in Photoproduction at HERA.* The European Physical Journal C5 (1998) 41-56
4. ZEUS Collaboration; J.Breitweg et al. *Search for Selectron and Squark Production in e^+p collisions at HERA.* Phys Letters B434 (1998) 214-230
5. ZEUS Collaboration; J.Breitweg et al. *Measurement of the Diffractive Cross Section in Deep Inelastic Scattering using ZEUS 1994 Data.* The European Physical Journal C6 (1999) 43-66
6. ZEUS Collaboration; J.Breitweg et al. *Measurement of inclusive $D^{*\pm}$ and associated dijet cross sections in photoproduction at HERA.* The European Physical Journal C6 (1999) 67-83
7. ZEUS Collaboration; J.Breitweg et al. *Measurement of Elastic Υ Photoproduction at HERA.* Physics Letters B 437 (1998) 432-444
8. ZEUS Collaboration; J.Breitweg et al. *Exclusive Electroproduction of ρ^0 and J/Psi Mesons at HERA.* The European Physical Journal C6 (1999) 603-627
9. ZEUS Collaboration; J.Breitweg et al. *ZEUS Results on the Measurement and Phenomenology of F_2 at low x and low Q^2.* The European Physical Journal C7 (1999) 609-630
10. ZEUS Collaboration; J.Breitweg et al. *Measurement of Three-jet Distributions in Photoproduction at HERA.* Physics Letters B 443 (1998) 394-408
11. ZEUS Collaboration; J.Breitweg et al., *Measurement of Jet Shapes in High Q^2 Deep Inelastic Scattering at HERA*, The European Physical Journal C8 (1999) 3, 367-380.
12. ZEUS Collaboration; J.Breitweg et al., *Forward Jet Production in Deep Inelastic Scattering at HERA*, The European Physical Journal C6 (1999) 239-252.
13. ZEUS Collaboration; J.Breitweg et al., *Exclusive Electroproduction of ρ^0 and J/ψ Mesons at HERA*, The European Physical Journal C6 (1999) 603-627.
14. ZEUS Collaboration; J.Breitweg et al., *ZEUS Results on the Measurement and Phenomenology of F_2 at Low x and Low Q^2*, The European Physical Journal C7 (1999) 609-630.
15. ZEUS Collaboration; J.Breitweg et al., *Measurement of Multiplicity and Momentum Spectra in the Current and Target Regions of the Breit Frame in Deep Inelastic Scattering at HERA*, The European Physical Journal C 11 (1999) 2, 251-270.

16. ZEUS Collaboration; J.Breitweg et al., *W Production and the Search for Events with an Isolated High-Energy Lepton and Missing Transverse Momentum at HERA*, Physics Letters B 471 (2000) 411-428

17. ZEUS Collaboration; J.Breitweg et al., *Measurement of High Q^2 Neutral Current e+p Deep Inelastic Scattering Cross Sections at HERA*, The European Physical Journal C 11 (1999) 3, 427-445.

18. ZEUS Collaboration; J.Breitweg et al., *Measurement of Dijet Photoproduction at High Transverse Energies at HERA*, The European Physical Journal C 11 (1999) 1, 35-50.

19. ZEUS Collaboration; J.Breitweg et al., *Search for Contact Interactions in Deep Inelastic $e^+p \rightarrow e^+X$ Scattering at HERA*, accepted by the European Physical Journal, MS 000121.

20. ZEUS Collaboration; J.Breitweg et al., *Measurement of High Q^2 Charged-Current e^+p Deep Inelastic Scattering Cross Sections at HERA*, The European Physical Journal C 12 (2000) 3, 411-428.

21. ZEUS Collaboration; J.Breitweg et al., *Angular and Current-Target Correlations in Deep Inelastic Scattering at HERA*, The European Physical Journal C 12 (2000) 1, 53-68.

22. ZEUS Collaboration; J.Breitweg et al., *Measurement of D^{*+-} production and the charm contribution to F_2 in deep inelastic scattering at HERA*, The European Physical Journal C 12 (2000) 1, 35-52.

23. ZEUS Collaboration; J.Breitweg et al. *Measurement of the Spin-Density Matrix Elements in Exclusive Electroproduction of ρ^0 Mesons at HERA*, The European Physical Journal C 12 (2000) 3, 393-410.

24. ZEUS Collaboration; J. Breitweg et al., *Measurement of diffractive photoproduction of vector mesons at large momentum transfer at HERA*, DESY 99-160 (October 1999), submitted to the European Physical Journal.

25. ZEUS Collaboration; J. Breitweg et al., *Measurement of inclusive prompt photon photoproduction at HERA*, DESY 99-161 (October 1999), accepted by Physics Letters B - PLB 15449 / WI 5057.

26. ZEUS Collaboration; J. Breitweg et al., *Measurement of the $E^2_{T,jet}/Q^2$ dependence of forward jet production at HERA*, Physics Letters B 474 (2000) 223-233.

27. ZEUS Collaboration; J. Breitweg et al., *The Q^2 Dependence of Dijet Cross Sections in γp Interactions at HERA*, DESY 00-017 (January 2000), accepted by Physics Letters B - ref. 5077.

28. ZEUS Collaboration; J. Breitweg et al., *Search for Resonances Decaying to e^{+-}jet in e^+p Interactions at HERA*, DESY 00-023 (February 2000), accepted by The European Physical Journal.

29. ZEUS Collaboration; J. Breitweg et al., *Measurement of Azimuthal Asymmetries in Deep Inelastic Scattering*, DESY 00-040 (March 2000), accepted by Physics Letters B - PLB 15927.

30. ZEUS Collaboration; J. Breitweg et al., *Measurement of Inclusive D_s^{+-} Photoproduction at HERA*, DESY 00-041 (March 2000), accepted by Physics Letters B - PLB 15928.

Contributions to the DESY MC Workshop, Hamburg, April 1998

"Monte Carlo generators for HERA physics", Hamburg 1998/1999.

1. N.H. Brook and L. Lonnblad, *Summary of activities in the Working Group on QCD Cascades*, 3-9.
2. N.H. Brook, T. Carli, E. Rodrigues, M.R. Sutton, N. Tobien and M. Weber, *A comparison of deep-inelastic scattering Monte Carlo event generators to HERA data*, 10-35.
3. N.H. Brook, *MLLA parton spectra compared to ARIADNE*, 51-57.
4. J.M. Butterworth, J. Chyla and G. Schuler, *Transition from Photoproduction to DIS - Introduction and Summary*, 197-202.
5. J.M. Butterworth and R.J. Taylor, *Global Comparisons of Jet Photoproduction Data and Monte Carlo*, 230-238.
6. Th. Hadig and G. McCance, *A common scheme for running NLO ep event generators*, 125-141.
7. G. McCance, *NLO program comparison for event shapes*, 151-159.

Contributions to the 3rd Durham Workshop on HERA Physics, Sept. 1998

J. Phys. G 25 no 7 (1999):

1. N.Brook, *Momentum spectra in the current region of the Breit frame in deep inelastic scattering at HERA*, 1445-1447.
2. P. Bussey, *Prompt photon production*, 1461-1464.
3. J.M.Butterworth (convenor), V.A.Khoze and W.Ochs, *soft particle emission accompanying dijet photoproduction*, 1457-1460.
4. J.E. Cole, *Recent experimental results in heavy flavour production at HERA*, 1371-1376.
5. A.M. Cooper-Sarkar et al., *High Q^2 deep inelastic scattering at HERA*, 1387-1409.
6. C.Cormack, *Measuring NC and CC DIS cross sections with e^- beams at HERA*.
7. C.Cormack, *Study of radiative corrections for high Q^2 DIS NC and CC.*
8. R. Devenish and W.J. Stirling, *Introduction*, 1269-1272.
9. M.E.Hayes and M.Kramer, *Heavy-Flavour Production at HERA*, 1477-1493.
10. J. Kalinowksi, M.W. Krasny and R. Walczak, *High E_T, exotics and rare processes – an introduction*, 1411.
11. K.R. Long et al., *High Q^2 Deep Inelastic Scattering at HERA*, 1387-1409.
12. T. Matsushita et al., *High p_T leptons and W production at HERA*, 1412-1417.

13. T. Matsushita, E. Perez and R. Rückl, *High Q^2 physics at HERA and searches for new particles*, 1418-1427.
14. C. Nath, R. Walczak and Y. Tamazaki, *Events with large E_T^{tot} in photoproduction at HERA*, 1440-1443.
15. L. Sinclair (convenor) et al., *Jet cross sections at HERA: current issues*, 1465-1469.
16. D.S. Waters, *Exotic and rare processes at HERA*, 1351-1359.

Contributions to the DIS1999 Workshop, Zeuthen, April 1999

1. A. Quadt, Structure Function Working group convenor and summary speaker.

Contributions to the Durham Workshop on Collider Physics, Sept. 1999

1. J.M.Butterworth, *QCD: How we can help each other.*
2. E.A.Heaphy, *Three-jet Production at HERA.*
3. M. Sutton, Heavy flavour group convenor.
4. M.R. Sutton, *Charm photoproduction and fragmentation at HERA.*

Popularisation

1. J.M.Butterworth, *HERA Electrons*, Frontiers issue 3, p7.
2. J.M.Butterworth, *Exploring the Quark*, Frontiers issue 6, p12.

B Conference Talks

Talks given at major national and international meetings in the period March 1998 to April 2000.

1. D. Bailey, *New ZEUS results on F_2^{charm}*, DIS98, Brussels, April 1998.
2. N. Brook, *QCD at HERA*, DIS98, Brussels, April 1998.
3. N. Brook, *QCD at HERA*, 2nd Latin American Symposium on High Energy Physics, Puerto Rico, 1998.
4. P. Bussey, *Physics with two photons at HERA*, Workshop on photon interactions and the photon structure, Lund, 1998.
5. J. Butterworth, *ZEUS results for Vancouver ICHEP98*, DESY Seminar, July 1998.
6. J. Butterworth, *Charm 'in' the photon*, Workshop on photon interactions and the photon structure, Lund, 1998.
7. A. Doyle, *Highlights and open questions from ZEUS*, DIS98, Brussels.
8. A. Doyle, *HERA physics*, IOP Conference on Particle Physics, Manchester, 1998.
9. A. Doyle, *Structure Functions*, ICHEP98, Vancouver, July 1998.
10. J. Gross-Knetter, *NC and CC cross sections at high Q^2 from ZEUS at HERA*, ICHEP98, Vancouver, July 1998.
11. R. Hall-Wilton, *Diffractive Heavy Flavour Production at HERA*, Small x and Diffractive Workshop, FNAL, September 1998.

12. G.D.Howell, *Measurement of the e^+p Charged Current Cross Section*, Proceedings of the 6th International Workshop on Deep Inelastic Scattering and QCD, Brussels, 4-6 April 1998, World Scientific.
13. K.R. Long, *Searches for New Physics at HERA*, Invited talk at the 1st International Conference 'From the Planck Scale to the Electroweak Scale', Kazimierz, May 1998.
14. A. Quadt, *Measurement of the neutral current e^+p cross section at $Q^2 > 400$ GeV^2 with the ZEUS detector at HERA*, Meeting of the German Physical Society (DPG), Freiburg, March 1998.
15. A. Quadt, *The ZEUS central tracking detector Second level trigger*, Meeting of the German Physical Society (DPG), Freiburg, March 1998.
16. A. Quadt, *Measurement and phenomenology of the proton structure function F_2 from ZEUS at HERA*, ICHEP98, Vancouver, July 1998.
17. A. Quadt, *The proton structure function F_2 at low and medium Q^2 at ZEUS*, (awarded the Giuseppe P.S. Occhialini scholarship for the best experimental presentation) International school of subnuclear physics, Erice, September 1998.
18. L.E. Sinclair, *Dynamics of multijet processes in photoproduction*, DIS'98, Brussels.
19. L.E. Sinclair, *Jets and prompt photons in photoproduction*, ICHEP XXIX, Vancouver, 1998.
20. M. Sutton, *Charm in photoproduction at HERA*, DIS98, Brussels, 1998.
21. R. Waugh, *Event shape variables in deep inelastic scattering*, DIS'98, Brussels.
22. M. Wing, *Photon structure and the hadronic final state in photoproduction at ZEUS*, Stara Lesna, Slovakia, 1998.
23. D. Bailey, *Measurement of the charm structure function of the proton*, The Structure of the Nucleon, Frascati, Italy, June 1999.
24. N. Brook, *Experimental results on Fragmentation and Event Shapes*, Workshop on New Results from HERA, Ringberg, June 1999.
25. P. Bussey, *Photoproduction at low Q^2*, Physics in Collision, Ann Arbor, 1999.
26. J.M. Butterworth, *Photon Structure*, Invited talk at Lepton-Photon 99, 18/8/99, Stanford Univ., USA.
27. J.M. Butterworth, R.J. Taylor, *A Global Study of Photon-Induced Jet Production*, Proceedings of Photon 99, Freiburg, Germany.
28. J.E. Cole, *Diffractive D^{*+-} (2010) Production in Deep Inelastic Scattering from ZEUS*, Proceedings of the 6th International Workshop on Deep Inelastic Scattering and QCD, Brussels, 4-6 April 1998, World Scientific.
29. A.M. Cooper-Sarkar, *Structure Functions at low Q^2*, Nucleon99, Frascati, June 1999.
30. R. Devenish, *Nucleon and Nuclear Structure Functions*, Workshop on Challenges in QCD, Kibbutz Kir Giladi, Israel, June 1999.
31. A.T. Doyle, *Event shapes and forward jet production at HERA*, Hadron 99, Beijing, 1999.
32. A.T. Doyle, *Physics at HERA*, CERN Academic Training Lectures, May 99.
33. A.T. Doyle, *Hadronic Final States*, Low-x Workshop, Tel Aviv, June 99.
34. J. Grosse-Knetter, *DIS at high Q^2*, German Physical Society, Heidelberg, March 1999.
35. J. Grosse-Knetter, *Deep Inelastic Scattering at High Q^2*, Proc. XIth Rencontres de

Blois, June 1999.

36. M.E. Hayes, *Heavy Flavours in Photoproduction at HERA*, Rencontres de Moriond on QCD and Hadronic Interactions 20-27 March 1999, Les Arcs, France.
37. S.W. Lee, *Prompt Photon Processes in Photoproduction at HERA*, International Conference on the Structure and Interactions of the Photon (*Photon99*), Freiburg, May 1999, Nucl. Phys. Proc. Suppl., Vol. 82, March 2000.
38. K.R. Long, *Future ep Physics: The Outlook for HERA*, 14th International Workshop on High Energy Physics and Quantum Field Theory, Moscow, 27 May - 2 June 1999.
39. K.R. Long, *Deep Inelastic Scattering at HERA*, Invited talk at the Institute of Physics Nuclear and Particle Physics Conference, Salford, 12-14 April 1999.
40. N. Macdonald, *Structure of real and virtual photons from ZEUS*, DIS 99, Zeuthen, 1999.
41. T. Matsushita, *W cross-section and events with high p_t leptons*, Moriond EW, March 1999.
42. N. McCubbin, *Low x, low Q^2 physics at HERA*, PANIC 99, Uppsala, Sweden, June 1999.
43. L. Sinclair (convenor) et al., *Progress and problems in QCD - report from the hadronic final states working group at DIS 99*, DIS 99, Zeuthen, 1999.
44. L. Sinclair, *Measurements of jet, single hadron and prompt photon photoproduction*, Workshop on New Results from HERA, Ringberg, June 1999.
45. N. Brook. *Physics at HERA*, IOP Conference on Particle Physics, Edinburgh, April 2000.
46. N. Brook, *The measurement of azimuthal asymmetries in DIS*, DIS2000, Liverpool, April 2000.
47. P. Bussey, *Inclusive prompt photoproduction and deeply virtual Compton scattering at HERA*, XXXV Rencontres de Moriond, Les Arcs, March 2000.
48. J. Cole, *Diffractive D^* production*, DIS2000, Liverpool, April 2000.
49. E. Heaphy, *Recent results in high E_T photoproduction*, DIS2000, Liverpool, April 2000.
50. S.W. Lee, *Prompt photons in photoproduction*, DIS2000, Liverpool, April 2000.
51. G. McCance, *Event shapes and correlations in the hadronic final state*, XXXV Rencontres de Moriond, Les Arcs, March 2000.
52. O. Ruske, *The Soft to pQCD Interface Region at HERA*, XXXV Rencontres de Moriond, Les Arcs, March 2000.
53. J. Scott, *Structure function at low Q^2 and x (the transition region)*, DIS2000, Liverpool, April 2000.

C UK Theses

(Submitted since PPESP report March 1998.)

1. H. Blaikley (Oxford, 1999) *Measurement of proton structure from the 1996 and 1997 radiative scattering data using the ZEUS detector.*

2. J. Bromley (Glasgow, 1998) *Measurement of fragmentation functions in DIS at HERA.*

3. J.E. Cole (Imperial, 1999) *Open Charm Production in deep inelastic diffractive ep scattering at HERA.*

4. J.K. Edmonds (Oxford, 1998) *Measurement of the NC DIS cross section at HERA using* e^+ *data from the ZEUS detector.*

5. R.J. Hall-Wilton (Bristol, 1999) *Diffractive and Non-Diffractive Charm Production in Deep Inelastic Scattering at HERA.*

6. M.E. Hayes (Bristol, 1998) *A Study of Parton-Parton Elastic Scattering by Colour Singlet Exchange.*

7. G.D. Howell (Imperial,1998) *Measurement of the Charged Current Cross-Section with the ZEUS Detector at HERA.*

8. N. Macdonald (Glasgow, 1999) *Structure of the virtual photon at HERA.*

9. C. Nath (Oxford, 1998) *Measurement of the inclusive jet cross section in high total transverse energy photoproduction at HERA.*

10. D. Piccioni (Bristol, 1999) *A Measurement of Elastic* ρ^0 *Production in* e^+p *Collisions.*

11. D.G. Roff (Bristol, 1998) *The Development of CVD Diamond Tracking Detectors for High Luminosity Experiments at the LHC and the Photon Structure of the Proton.*

12. D. Sideris (Imperial,1998) *Measurement of the charm contribution to the proton structure function at HERA.*

13. E.J. Strickland (Glasgow, 1998) *A first study of multijet dynamics in hard photoproduction at HERA.*

14. M.R. Sutton (UCL, 1998) *Charm in Dijet Photoproduction at HERA.*

15. D.S. Waters (Oxford, 1998) *A first estimate of* $\sigma(e^+p \to e^+W^\pm X)$ *and studies of high* p_T *leptons with the ZEUS detector at HERA.*

16. R. Waugh (Glasgow, 1999) *Measurement of event shape variables using the current region of the Breit frame in deep inelastic scattering.*

17. M. Wing (UCL, 1999) *The Study of Heavy Quark Production in High* E_T *Photoproduction at HERA using the ZEUS Detector.*

D ZEUS UK Collaboration

Academic staff, RAs and post-doctoral fellows, students in post 1st March 2000.

Bristol University D. S. Bailey, O. Barret[1], N. H. Brook, B. Foster, G. P. Heath, H. F. Heath, J. P. Scott[1], E. Rodrigues[1], S. Robins[1], R. J. Tapper

Glasgow University M. Bell[1], P. Bussey, A. Doyle, C. Glasman, S. W. Lee[1], A. Lupi, G. McCance[1], D. Saxon, I. Skillicorn

Imperial College London R. Goncalo[1], K. R. Long, F.Metlica, A. Tapper[1], R. Walker

Oxford University S. Boogert[1], A. M. Cooper-Sarkar, R. C. E. Devenish, J. Grosse-Knetter(10%), T. Matsushita, M. Rigby[1], O. Ruske[1], M. Sutton, R. Walczak

Rutherford Appleton Laboratory C. M. Cormack, J. C. Hart, N. A. McCubbin, T. P. Shah

University College London J. M. Butterworth, C. Gwenlan[1], M. E. Hayes, E. A. Heaphy[1], T. W. Jones, J. B. Lane, B. J. West[1]

We are grateful to the engineers and support staff at the ZEUS UK institutes, who have provided invaluable help. For help over the past two years we would particularly like to acknowledge:

Bristol: J-P. Melot, S. Nash,
Glasgow: A. J. Flavell
Imperial: A. K. Jamdagni, D. G. Miller, G. Barber, P. Savage, L. Toudup, I. Clarke, S. Greenwood
UCL: T. J. Fraser, D. A. Hayes, G. Nixon, M. Postranecky
Oxford: M. Dawson, P. D. Gronbech, T. Handford, G. Harris, J. Hill, I. McArthur, P. Shield, C. Sutton, S. Topp-Jorgensen
RAL: J. D. Baker, D. J. Ballard, D. J. Beckett, I. Church, C. J. Croxford, C. P. Day, S. B. Galagedera, M. D. Gibson, R. Halsall, J. Hartley, R. Hatley, G. Johnson, R. Matson, M. C. Morrissey, B. T. Payne, S. P. H. Quinton, R. L. Thompson, D. S. Wilsher

[1] Graduate Student

E Staff Allocations

The table shows the planned strength of ZEUS in % FTE for each year (Oct.-Sept.)

Name	00/01	01/02	02/03	03/04
Bristol:				
N.H. Brook	45	45	45	45
B. Foster	90	90	90	50
G.P. Heath	5	5	5	5
H.F. Heath	10	10	10	10
R.J. Tapper	20	20	20	20
D.S. Bailey	30	50	50	50
A.N. Other	100	100	100	100
Glasgow:				
P.J. Bussey	25	25	25	25
A.T. Doyle	70	70	60	10
D.H. Saxon	10	50	25	25
I.O. Skillicorn	60	40	30	20
C. Glasman	100	100	100	100
A. Lupi	100	100	100	100
Imperial:				
K. Long	90	80	60	50
R. Walker	100	75	50	50
F. Metlica	100	100	(100)*	(100)*
Oxford:				
R.C.E. Devenish	50	50	40	40
R. Walczak	50	50	40	40
A.M. Cooper-Sarkar	40	40	40	30
J. Grosse-Knetter	10			
T. Matsushita	100	100	100	100
M. Sutton	100	100	100	100
RAL:				
J. Hart	90	80	70	70
N.A.M. McCubbin	10	10	10	10
C. Cormack	100	50		
UCL:				
J.M. Butterworth	30	30	30	30
T.W. Jones	30	30	30	30
J.B. Lane	40	30	10	
M.E. Hayes	100	100	100	100

Posts in italics are Research Associates

* Responsive R.A. post (subject to additional funding)

F Computing Requirements

ZEUS-UK represents 14% of the total non-student effort on ZEUS and currently generates approximately 8% of the total Monte Carlo production for the experiment. RAL Central computing is also used for NLO Monte Carlo generation. We anticipate CPU, networking and disk space requirements to increase by a factor of two, averaged over the next two years, yielding the following estimates: CPU at 80 SpecInt95 under linux, networking to DESY at 0.2 Mbit/sec, disk usage for intermediate storage at less than 100 Gbytes and minimal tape usage.

G ZEUS Organisation

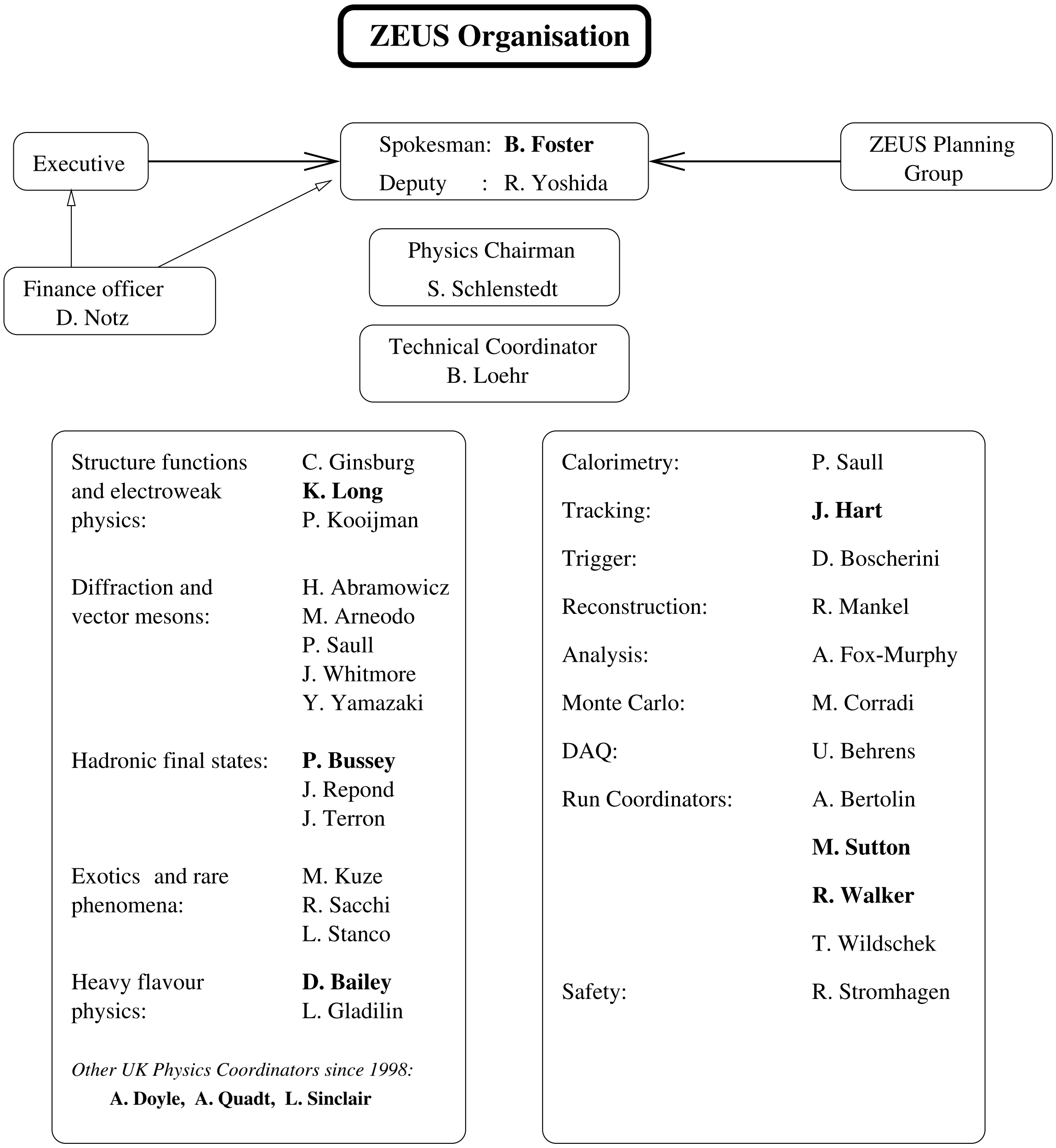

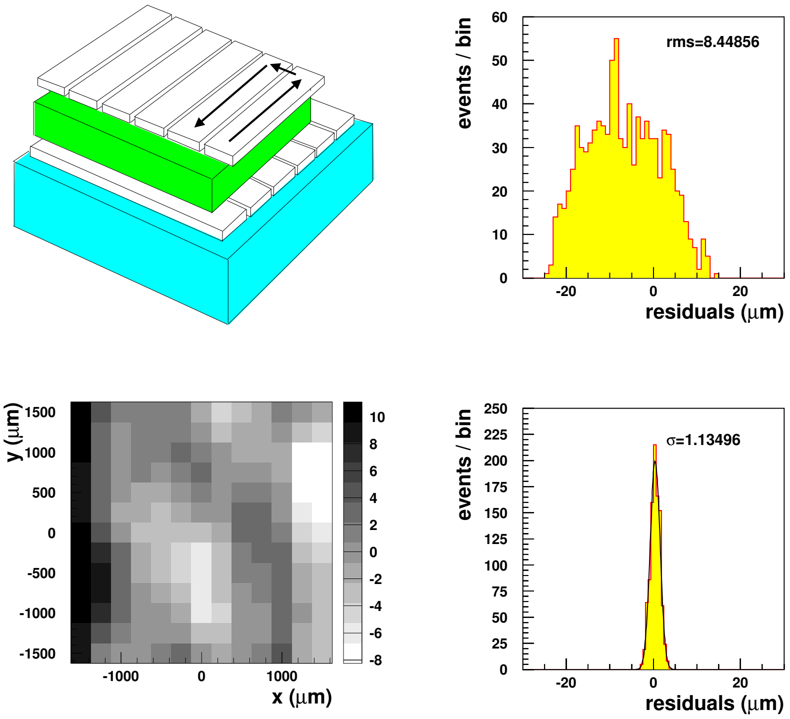

Figure 1: Improvement in precision of the laser beam position measurement after calibration of the sensor. The figure shows the calibration 'map' (lower LH plot) and the improvement in the resolution from 8.4 μm to 1.1 μm.

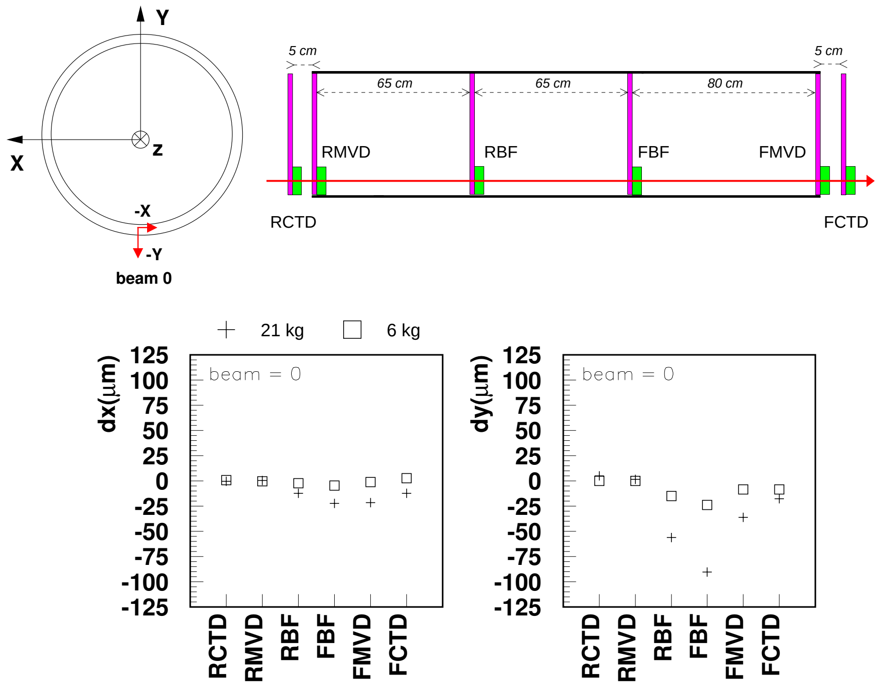

Figure 2: Online plots from the optical alignment test at NIKHEF, December 1999. The figure shows the positions of the sensors and laser beam on the MVD support tube and the deviation in the sensor local coordinate system when an even loading was applied to the tube.

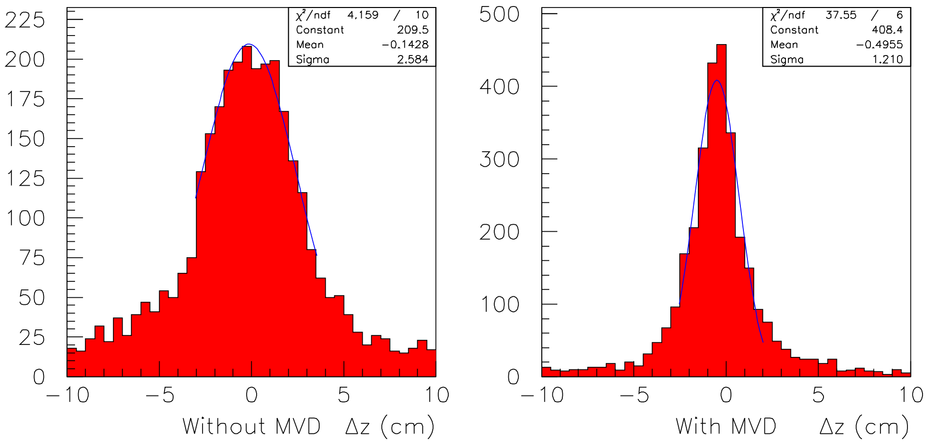

Figure 3: The single track z-vertex resolution of the CTD SLT algorithm using only CTD information (left plot) and using the MVD information to guide CTD stereo hit matching (right plot).

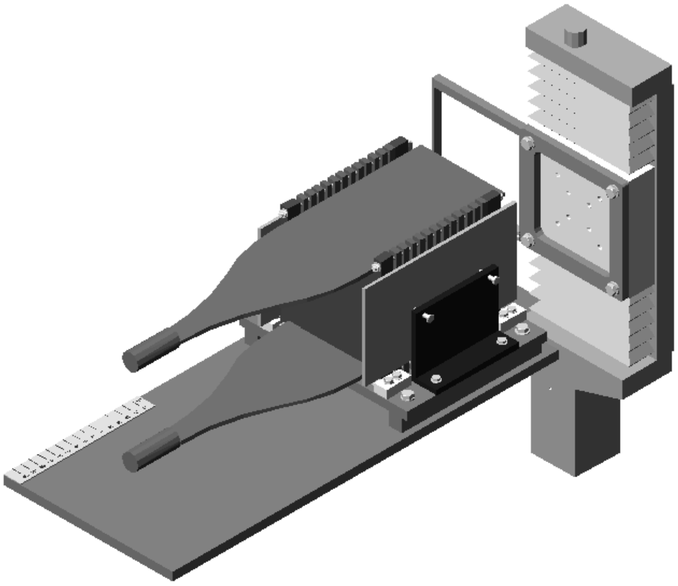

Figure 4: Schematic diagram of the TPOL calorimeter showing the calorimeter and the top and bottom scintillation counters. The precision stage is shown together with the scintillating fibre support structure. The silicon mitristrip detector would be mounted directly on the front face of the calorimeter using existing bolts. In operation the scintillating fibre would be moved vertically across the silicon detector periodically.

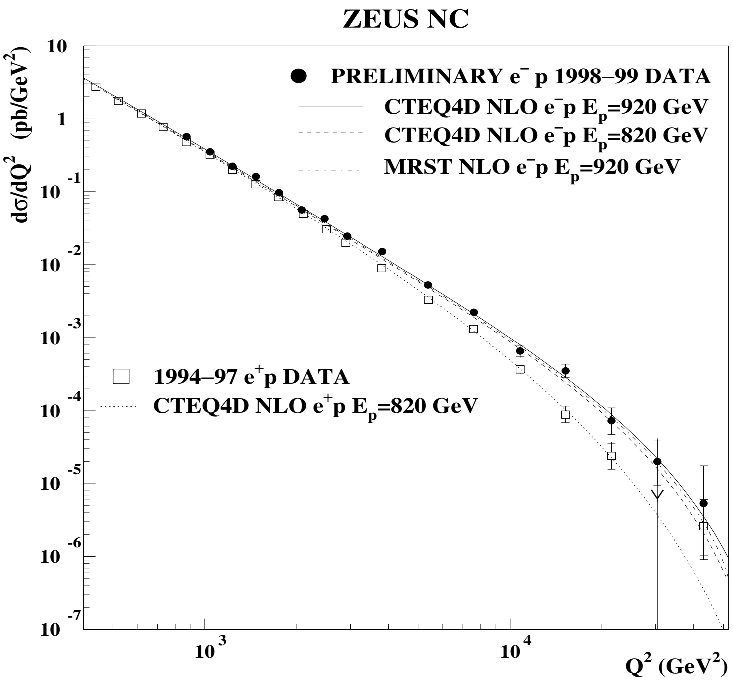

Figure 5: Differential e^+p and e^-p $d\sigma/dQ^2$ cross sections compared to the Standard Model predictions from CTEQ4D (solid line) and MRST (dashed line).

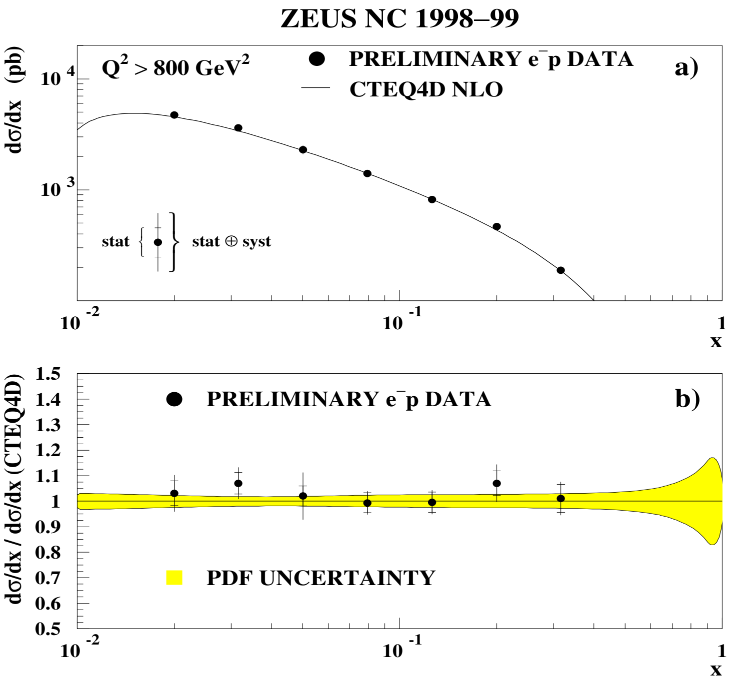

Figure 6: Differential e^+p and e^-p $d\sigma/dx$ cross section for $Q^2 > 800\,\mathrm{GeV}^2$ compared to the Standard Model predictions from CTEQ4D (solid line) and the PDF uncertainty estimated by ZEUS (shaded band).

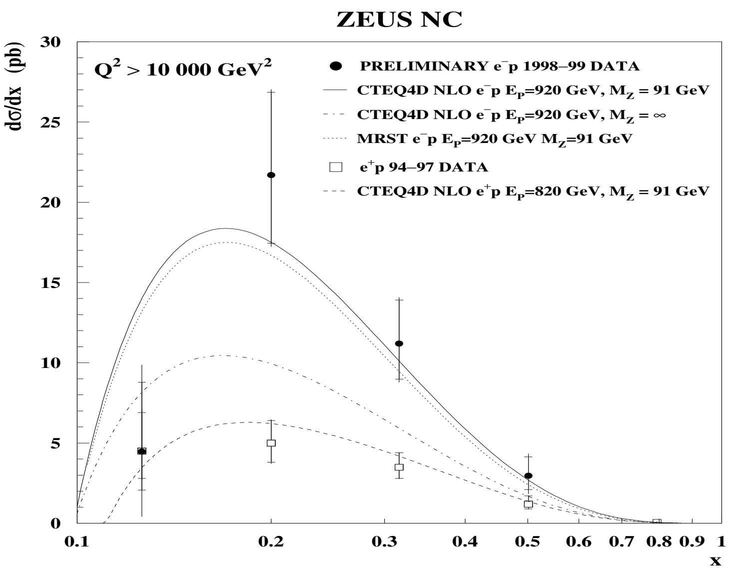

Figure 7: Differential e^+p and e^-p $d\sigma/dx$ cross section for $Q^2 > 10\,000\,\mathrm{GeV}^2$ compared to the Standard Model predictions from CTEQ4D (solid line) and MRST (dashed line).

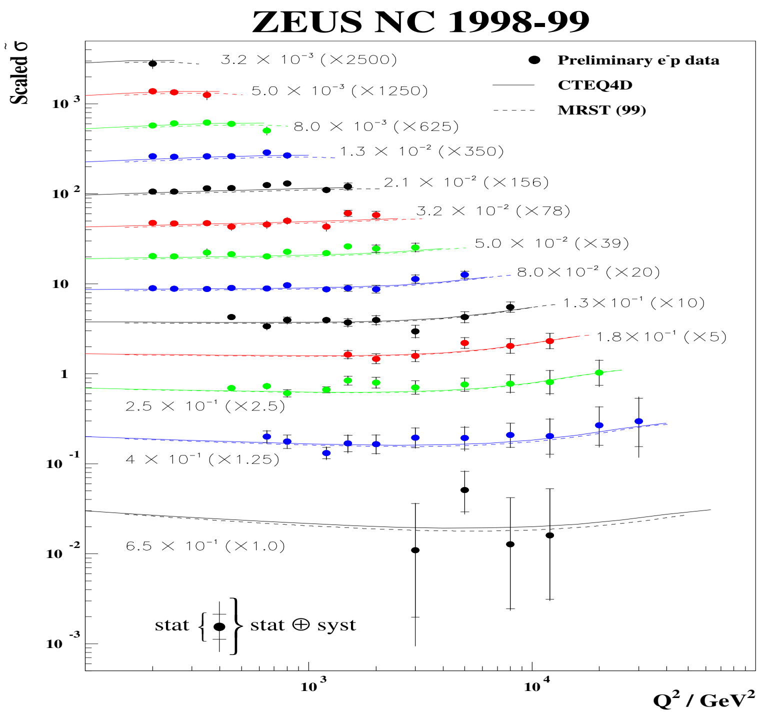

Figure 8: The reduced e^-p cross section compared to the Standard Model predictions from CTEQ4D (solid line) and MRST (dashed line). For high values of $x > 0.18$ the e^-p data is seen to rise at high values of Q^2, as opposed to the e^+p data which turns down at large values of Q^2.

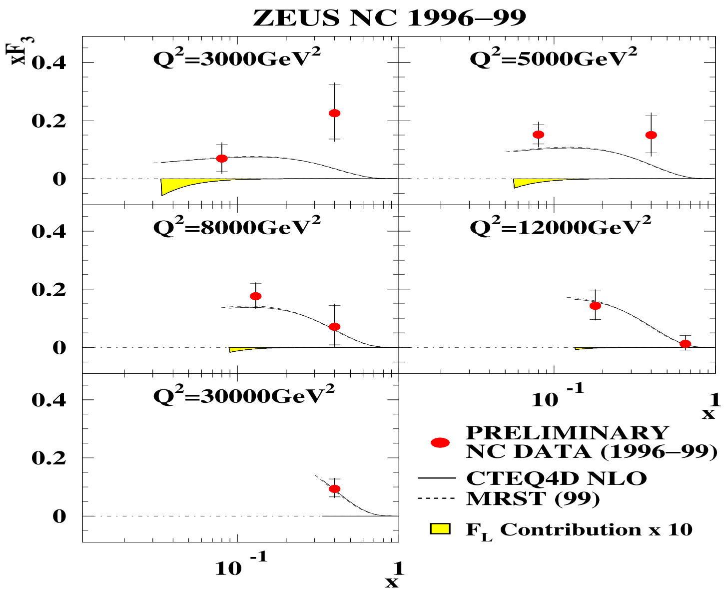

Figure 9: Extraction of xF_3 at fixed Q^2 as a function of x compared to the Standard Model predictions from CTEQ4D (solid line) and MRST (dashed line). The shaded band shows the correction of F_L to the expected value of xF_3 scaled by a factor of 10.

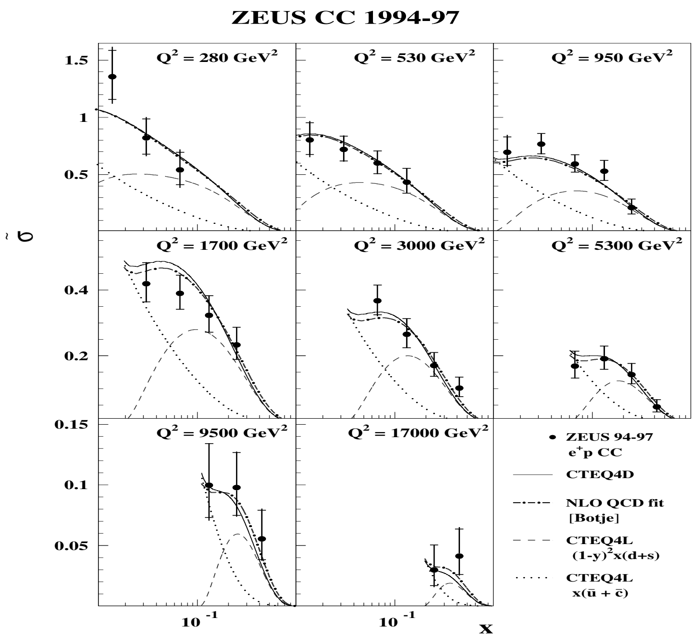

Figure 10: The reduced cross section $\tilde{\sigma}$ for e^+p CC DIS as a function of x, for fixed values of Q^2. The dots represent the data, while the expectations of the Standard Model evaluated using the CTEQ4D PDFs are shown as the solid lines. For illustration, the leading-order PDF combinations $x(\bar{u}+\bar{c})$ and $(1-y)^2x(d+s)$, taken from the CTEQ4L parameterization, are plotted as dotted and dashed lines, respectively. Also shown is the result of the ZEUS NLO QCD fit (dash-dotted line).

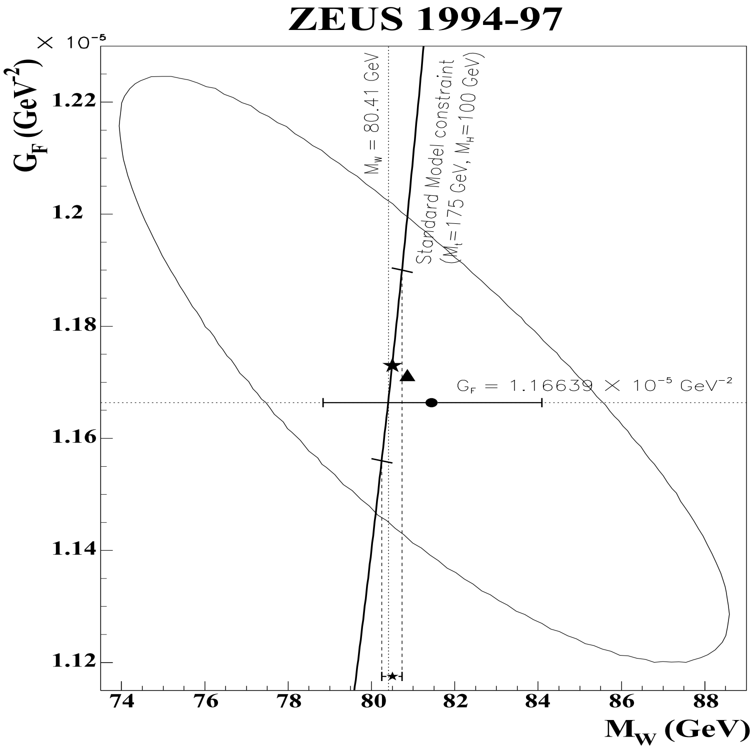

Figure 11: The result of a fit of the CC DIS cross section to determine G_F and M_W. The triangle indicates the result of the fit, i.e. the position of $\chi^2_{\rm min}$, the minimum value of χ^2. The 70% confidence level contour is shown as the ellipse. The dot with error bar shows the result of the 'propagator-mass' fit, described in the text, in which the χ^2 function is evaluated along the horizontal line $G_F = 1.16639 \times 10^{-5}\,\mathrm{GeV}^{-2}$. The SM relation between G_F and M_W is shown as the heavy solid line. The large star shows the position of $\chi^2_{\rm min}$(SM), the minimum of the χ^2 function evaluated along the SM constraint line. The solid bars crossing the SM constraint line show where $\chi^2(\mathrm{SM}) = \chi^2_{\rm min}(\mathrm{SM}) + 1$. The small star at the bottom with the error bar shows the value of M_W obtained in the 'Standard Model fit'. Note that all errors and the confidence level contour correspond to statistical errors only. Also shown (dotted) are lines of constant G_F (1.16639×10^{-5} GeV^{-2}) and constant M_W (80.41 GeV).

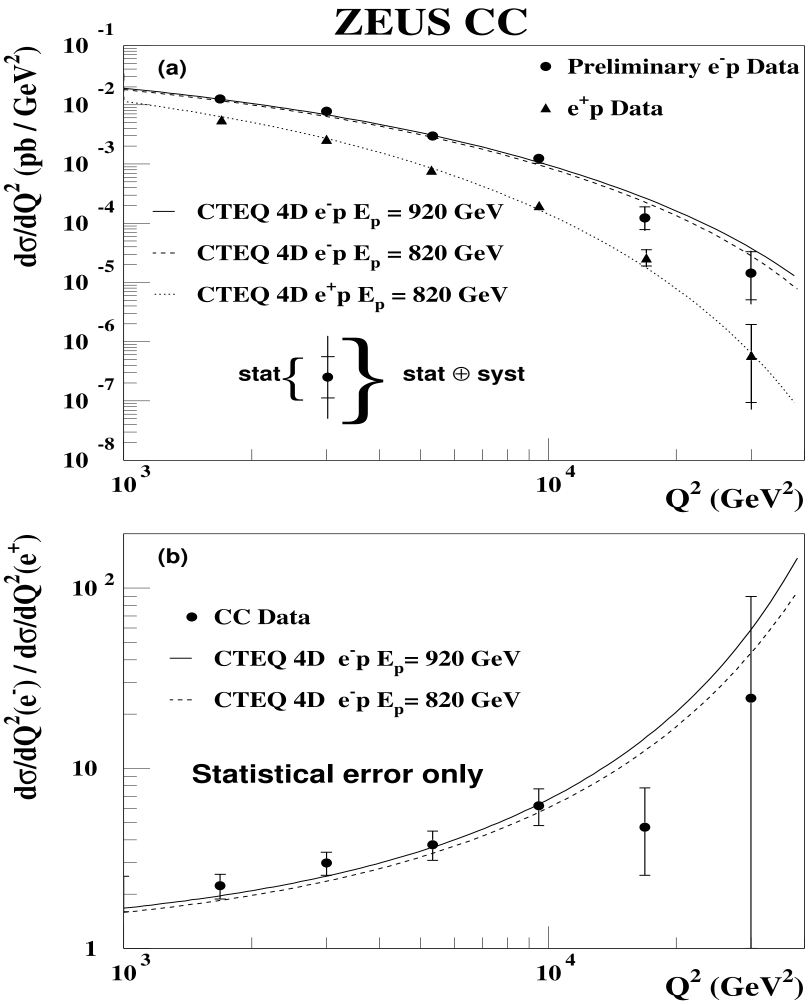

Figure 12: (a) Comparison of the differential cross sections $d\sigma/dQ^2$ for e^+p and e^-p CC DIS from ZEUS. (b) The ratio of the differential cross sections. The lines represent the SM predictions evaluated using CTEQ4D PDFs.

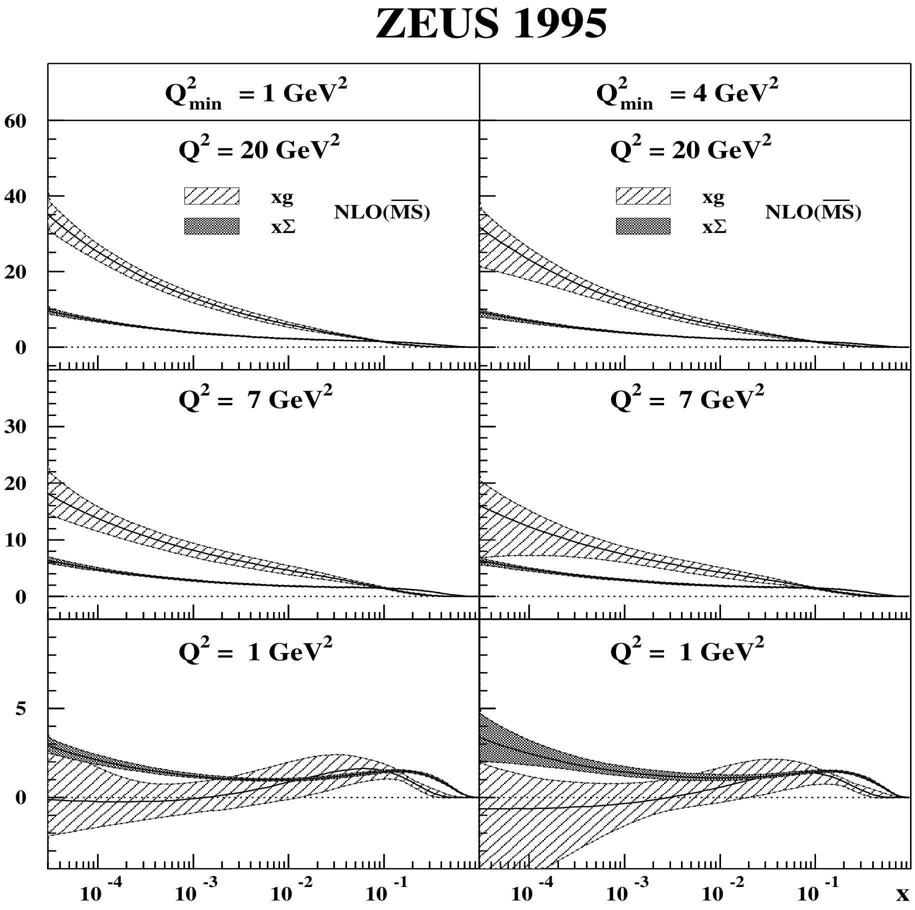

Figure 13: The quark singlet momentum distribution, $x\Sigma$ (shaded), and the gluon momentum distribution, $xg(x)$ (hatched), as functions of x at fixed values of $Q^2 = 1$, 7 and 20 GeV^2 from the ZEUS QCD fit. The error bands correspond to the quadratic sum of all error sources considered for each parton density. The three left-hand (right-hand) plots show the results from the standard fit including F_2 data with $Q^2 > 1$ GeV^2 (4 GeV^2).

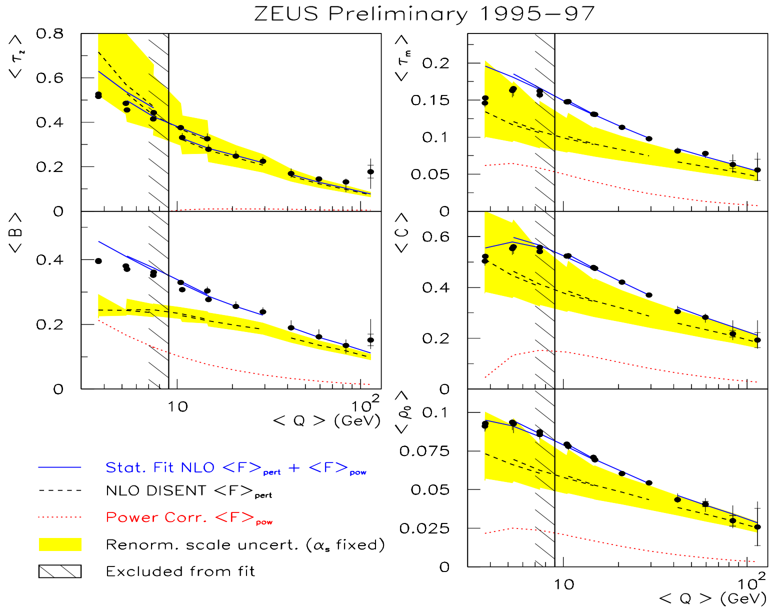

Figure 14: ZEUS preliminary mean event shape variables versus Q compared to two-parameter fits using the NLO calculation plus power correction approach described in the text. The shaded region represents the renormalisation scale uncertainty where $Q/2 < \mu_R < 2Q$, with α_S fixed to the fitted value.

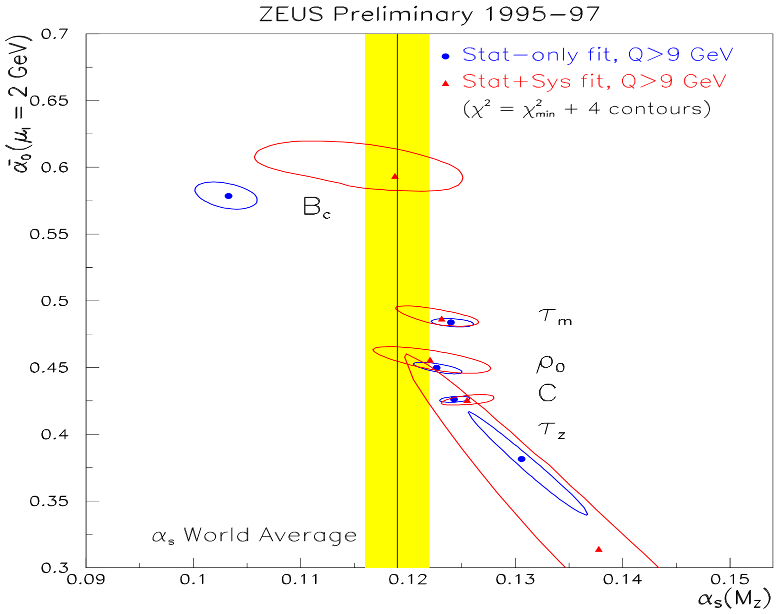

Figure 15: ZEUS preliminary contour plot of two-parameter fits of $\overline{\alpha}_0(\mu_I)$ and $\alpha_s(M_Z)$ to mean event shape variables. 2σ stat and stat$\oplus$sys contours for τ, B, τ_C, ρ and C parameters are indicated.

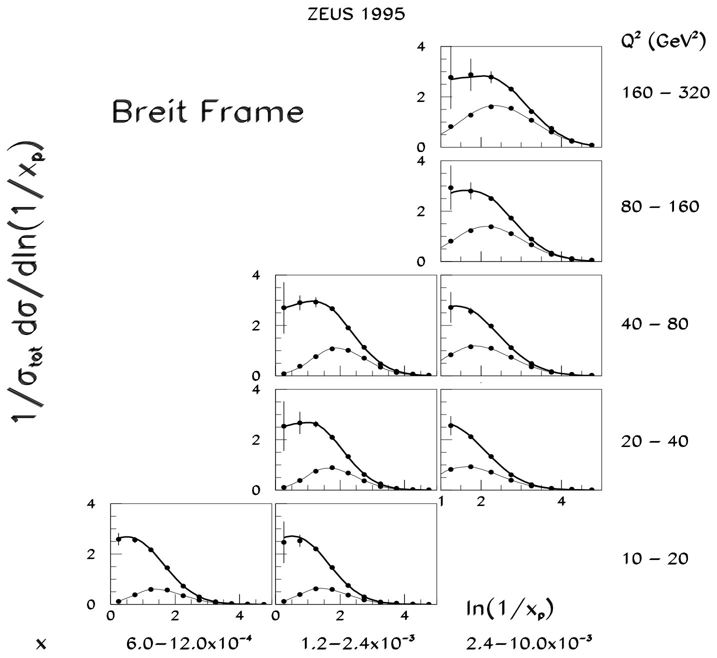

Figure 16: The corrected $\ln(1/x_p)$ distributions for the target and current regions for the 1995 data. Fitted two-piece normal distributions are shown to guide the eye. The heavy line corresponds to the target region, the light line to the current region. The error bars are the sum of the statistical and systematic errors in quadrature.

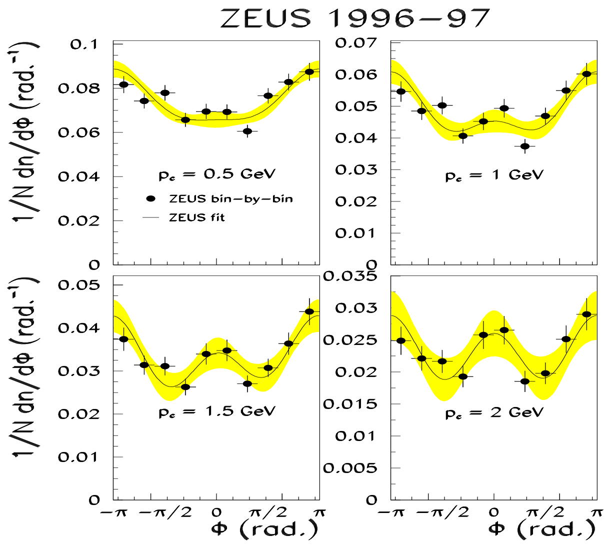

Figure 17: The differential ϕ distributions obtained for four values of the p_T cut, p_c, in the hadronic centre-of-mass frame in the kinematic region $0.01 < x < 0.1$ and $0.2 < y < 0.8$ for charged hadrons with $0.2 < z_h < 1.0$. The full line (with accompanying statistical error band) is the result obtained from the main analysis using the unfolding technique. The data points were corrected using a bin-by-bin procedure (only statistical errors are shown).

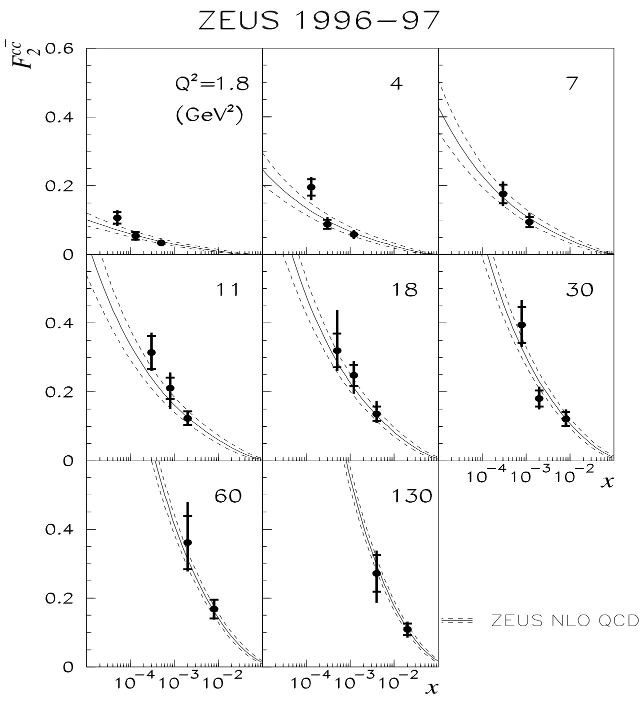

Figure 18: F_2^c as a function of x at fixed Q^2.

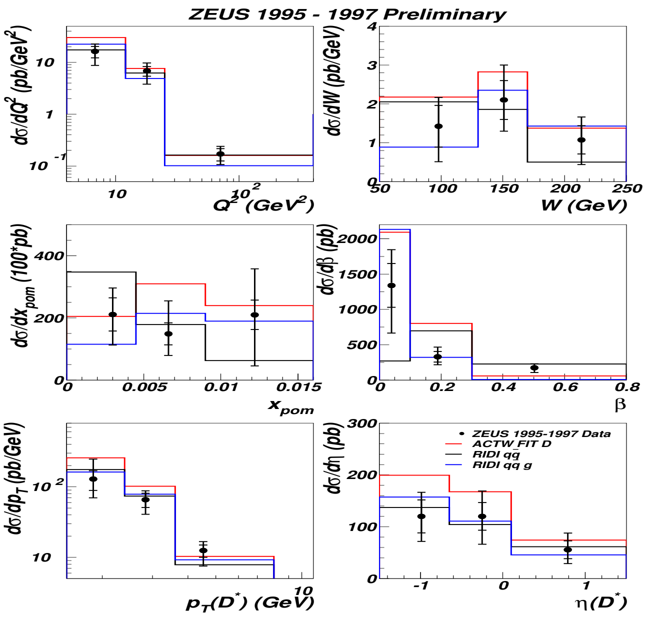

Figure 19: The differential D^* cross sections as functions of Q^2, W, x_{pom}, β, $p_t^{D^*}$ and η_{D^*} compared to theoretical predictions. The points show the ZEUS data. The inner error bar shows the statistical error and the outer bar the statistical and systematic errors added in quadrature.

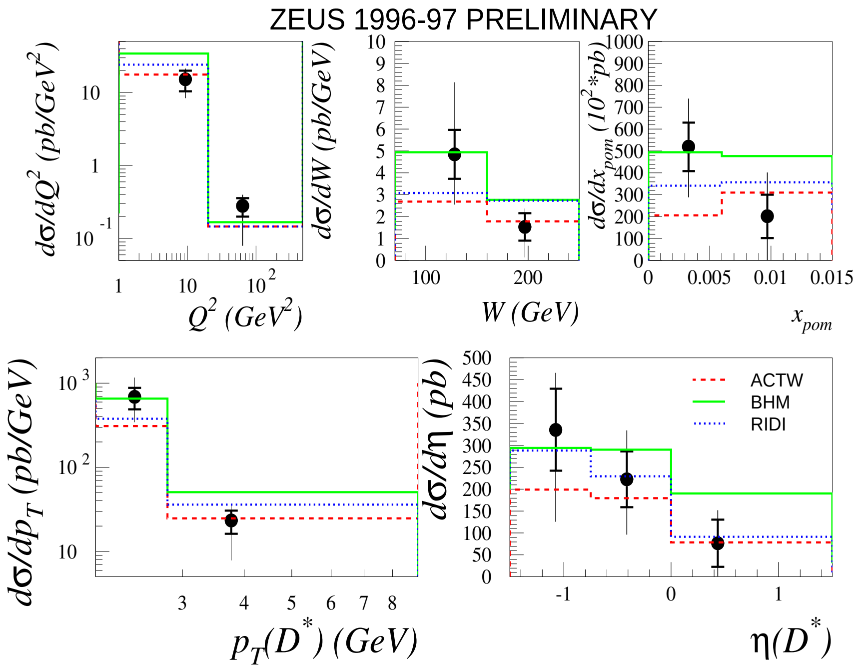

Figure 20: The differential D^* cross sections measured using the $D^* \to D^0\pi$, $D^0 \to K\pi\pi\pi$ decay as functions of Q^2, W, x_{pom}, $p_t^{D^*}$ and η_{D^*} compared to theoretical predictions. The points show the ZEUS data. The inner error bar shows the statistical error and the outer bar the statistical and systematic errors added in quadrature.

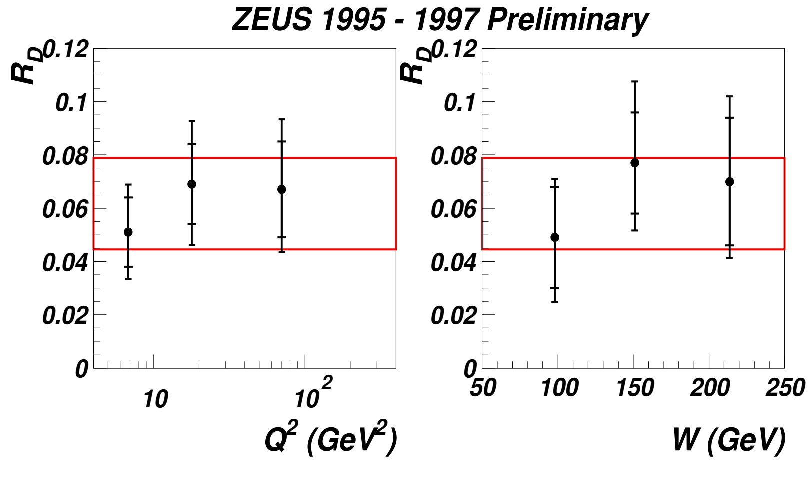

Figure 21: The ratio of diffractively produced D^* mesons to total D^* mesons. The left plot shows the ratio as a function of Q^2 and the right plot the ratio as a function of W. The inner error bars indicate the statistical error and the outer bar the statistical and systematic uncertainties added in quadrature. The measured ratio and its error are indicated by the horizontal lines.

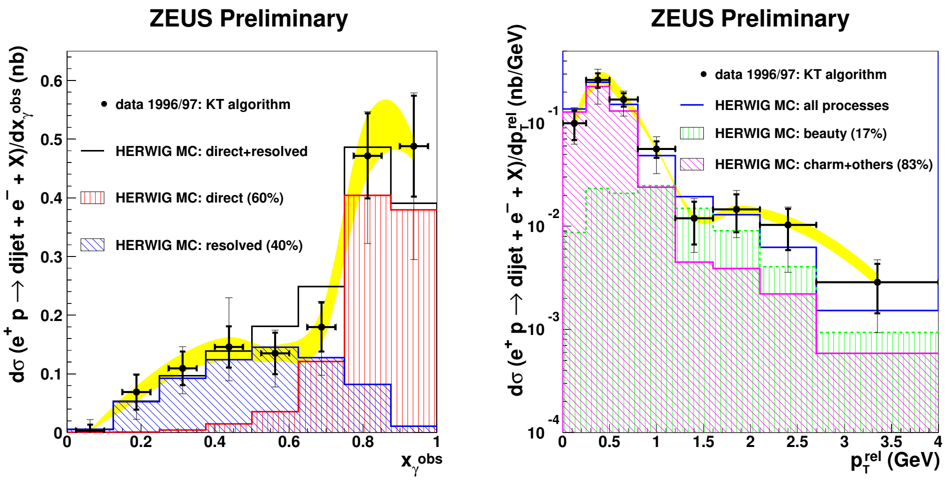

Figure 22: (a) The $x_\gamma^{\rm OBS}$ distribution for heavy flavour decays tagged with an electron, confirming the presence of a resolved component. (b) The transverse momentum of the electron relative to the jet axis, showing the presence of beauty quarks.

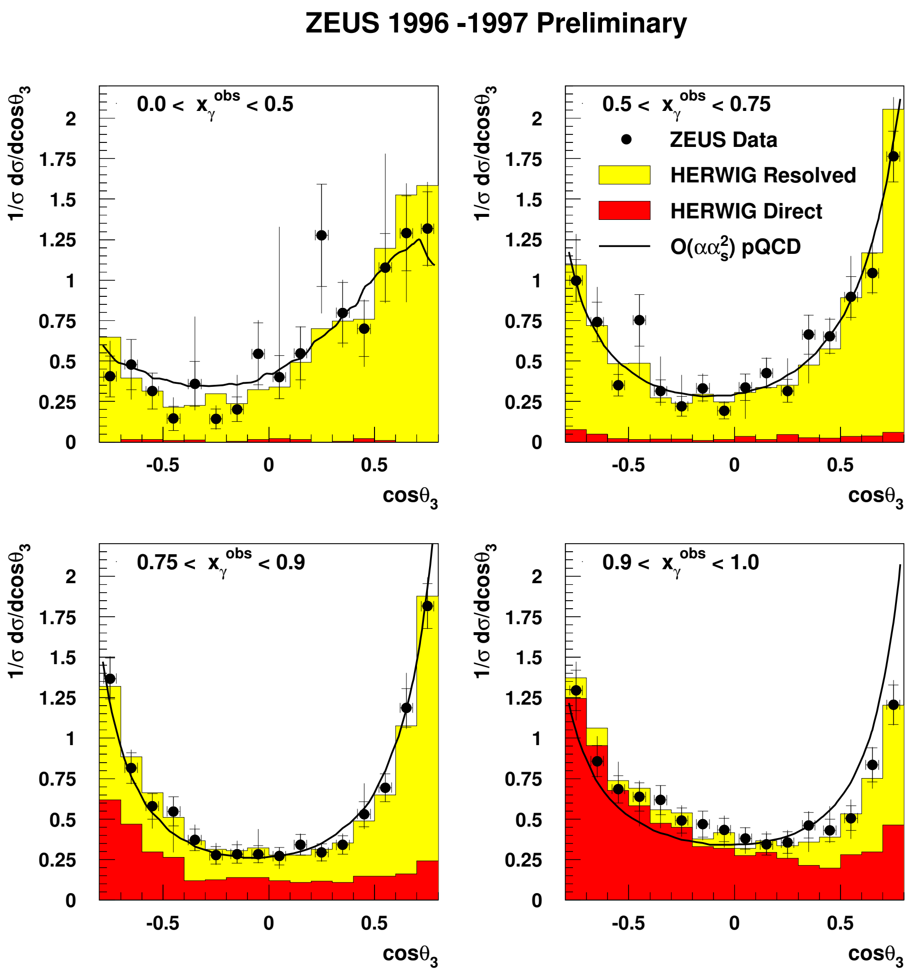

Figure 23: ZEUS preliminary three jet cross sections. LO resolved photon processes are shown by light shading, and LO direct by dark shading.

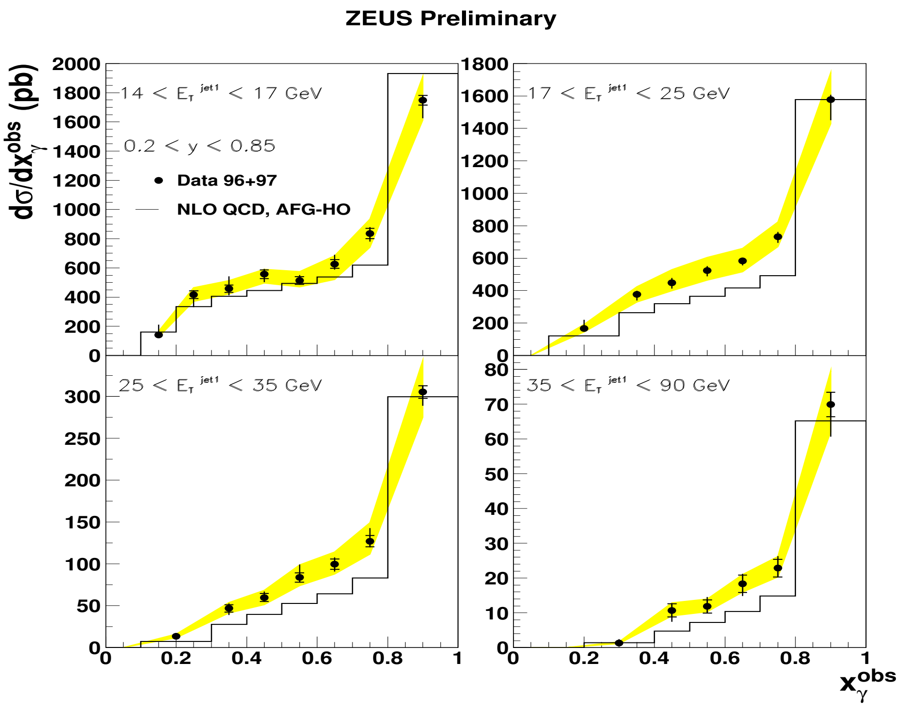

Figure 24: ZEUS preliminary jet cross sections compared to the NLO QCD calculation of Frixione and Ridolfi. The shaded area indicates the hadronic energy-scale uncertainty.

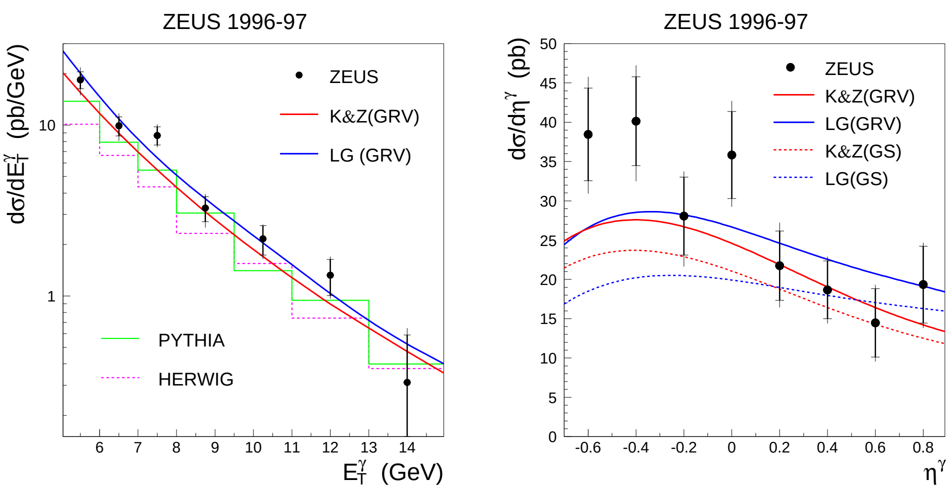

Figure 25: (a) E_T distribution of prompt photons in ZEUS (left plot), (b) pseudorapidity distribution (right plot).